

FINAL REPORT
DEVELOPMENT OF ADVANCED
FUEL CELL SYSTEM

By

B. Gitlow
A. P. Meyer
W. F. Bell
R. E. Martin

6 June 1978

UNITED TECHNOLOGIES CORPORATION
Power Systems Division

Prepared for

NATIONAL AERONAUTICS AND SPACE ADMINISTRATION

NASA Lewis Research Center

Contract NAS3-19778

Dr. L. H. Thaller, Project Manager

(NASA-CR-159443) DEVELOPMENT OF ADVANCED FUEL CELL SYSTEM Final Report, 25 Feb. - 31 Dec. 1976 (United Technologies Corp.) 74 p CSCL 10A
HC A04/MF A01
N79-12553
Unclas
G3/44 38852

REPRODUCED BY
NATIONAL TECHNICAL
INFORMATION SERVICE
U.S. DEPARTMENT OF COMMERCE
SPRINGFIELD, VA. 22161

NOTICE

This report was prepared as an account of Government-sponsored work. Neither the United States, nor the National Aeronautics and Space Administration (NASA), nor any person acting on behalf of NASA:

- (A) Makes any warranty or representation, expressed or implied, with respect to the accuracy, completeness, or usefulness of the information contained in this report, or that the use of any information, apparatus, method, or process disclosed in this report may not infringe upon privately-owned rights; or
- (B) Assumes any liabilities with respect to use of, or for damages resulting from the use of, any information, apparatus, method or process disclosed in this report.

As used above, "person acting on behalf of NASA" includes any employees or contractor of NASA, or employee of such contractor, to the extent that such employee or contractor of NASA or employee of such contractor prepares, disseminates, or provides access to any information pursuant to this employment or contract with NASA, or his employment with such contractor.

FINAL REPORT
DEVELOPMENT OF ADVANCED
FUEL CELL SYSTEM

By

B. Gitlow
A. P. Meyer
W. F. Bell
R. E. Martin

6 June 1978

UNITED TECHNOLOGIES CORPORATION
Power Systems Division

Prepared for

NATIONAL AERONAUTICS AND SPACE ADMINISTRATION

NASA Lewis Research Center
Contract NAS3-19778

Dr. L. H. Thaller, Project Manager

ASA-CR-159443) DEVELOPMENT OF ADVANCED N79-12553
EL CELL SYSTEM Final Report, 25 Feb. - 31
c. 1976 (United Technologies Corp.) 74 p
A04/MF A01 CSSL 10A Unclas
G3/44 38852

REPRODUCED BY
NATIONAL TECHNICAL
INFORMATION SERVICE
U.S. DEPARTMENT OF COMMERCE
SPRINGFIELD, VA. 22161

NOTICE

This report was prepared as an account of Government-sponsored work. Neither the United States, nor the National Aeronautics and Space Administration (NASA), nor any person acting on behalf of NASA:

- (A) Makes any warranty or representation, expressed or implied, with respect to the accuracy, completeness, or usefulness of the information contained in this report, or that the use of any information, apparatus, method, or process disclosed in this report may not infringe upon privately-owned rights; or
- (B) Assumes any liabilities with respect to use of, or for damages resulting from the use of, any information, apparatus, method or process disclosed in this report

As used above, "person acting on behalf of NASA" includes any employees or contractor of NASA, or employee of such contractor, to the extent that such employee or contractor of NASA or employee of such contractor prepares, disseminates, or provides access to any information pursuant to this employment or contract with NASA, or his employment with such contractor

NOTICE

THIS DOCUMENT HAS BEEN REPRODUCED FROM THE BEST COPY FURNISHED US BY THE SPONSORING AGENCY. ALTHOUGH IT IS RECOGNIZED THAT CERTAIN PORTIONS ARE ILLEGIBLE, IT IS BEING RELEASED IN THE INTEREST OF MAKING AVAILABLE AS MUCH INFORMATION AS POSSIBLE.

FINAL REPORT
DEVELOPMENT OF ADVANCED
FUEL CELL SYSTEM

By

B. Gitlow
A P Meyer
W. F Bell
R E Martin

6 June 1978

UNITED TECHNOLOGIES CORPORATION
Power Systems Division

Prepared for
NATIONAL AERONAUTICS AND SPACE ADMINISTRATION
NASA Lewis Research Center
Contract NAS3-19778
Dr L. H. Thaller, Project Manager

FOREWORD

This final report describes the research and development tasks performed during an advanced fuel cell technology program.

The work was performed under a NASA Contract NAS3-19778 from 25 February 1976 through 31 December 1976. The NASA Program Manager for this contract was Dr. Lawrence H. Thaller. The contributions of Dr. Thaller, Mr. Paul R. Prokopius and other members of the Direct Energy Conversion Laboratory staff at the NASA Lewis Research Center are gratefully acknowledged.

Principal Power Systems Division personnel who directed the tasks performed in this program were

B. Gitlow
A. P. Meyer
W. F. Bell

TABLE OF CONTENTS

	Page
Foreword	ii
Table of Contents	iii
List of Illustrations	iv
List of Tables	vi
Abstract	vii
I Summary	1
II Introduction	3
III Single Cell Fabrication & Testing	5
A. Single Cell Design	5
B. Single Cell Test Results	7
IV Two-Cell Plaque Fabrication & Testing	29
A Two Cell Plaque Design	29
B Two-Cell Plaque Test Results	30
Appendix A Base Cell Electrolyte Loss	
Appendix B. Electrolyte Reservoir Plate Improvement Program	
Appendix C. NASA Distribution List	
References	

ILLUSTRATIONS

No	Title	Page
1	Performance History, Single Cell No 42	8
2	Anode Diffusion Loss Comparison	9
3	Electrolyte Excursion Data, Single Cell No. 42	11
4	Electrolyte Conversion to Carbonate, Single Cell No. 42	11
5	Performance History, Single Cell No 44	13
6	Electrolyte Conversion to Carbonate, Single Cell No. 44	15
7	Electrolyte Excursion Data, Single Cell No 44	15
8	Cross Section, Single Cell No. 45	17
9	Performance History, Single Cell No 45	19
10	Electrolyte Excursion Data, Single Cell No 45	20
11	Electrolyte Excursion Data, Single Cell No 45	21
12	Electrolyte Excursion Data, Single Cell No 45	22
13	Electrolyte Excursion Data, Single Cell No 45	23
14	Cross Section, Single Cell No 46	24
15	Performance History, Single Cell No 46	25
16	Electrolyte Excursion Data, Single Cell No. 46	25
17	Electrolyte Excursion Data, Single Cell No 46	26
18	Electrolyte Excursion Data, Single Cell No. 46	27
19	Two Cell Plaque Test Setup	29
20	Performance History, Two-Cell Plaque No 1	31
21	Two Cell Plaque No 1	33
22	Performance History, Two-Cell Plaque No. 2	34
23	Two-Cell Plaque Voltage Connections Showing Flow Field Shorted to Anodes	36
24	Electrolyte Excursion Data, Two-Cell Plaque No. 2, Cell No 1	37
25	Electrolyte Excursion Data, Two-Cell Plaque No. 2, Cell No. 2	37
26	Electrolyte Excursion Data, Two-Cell Plaque No 2, Cell No. 1	39
27	Electrolyte Excursion Data, Two-Cell Plaque No. 2, Cell No. 2	39
28	Two-Cell Plaque No. 2, Wet Side Electrolyte Excursion	40
29	Cross Section of Two-Cell Plaque No. 3 Showing Adjustable Pinch Feature	41
30	Performance History, Two-Cell Plaque No.3	42
31	Electrolyte Excursion Data Two-Cell Plaque No. 3, Cell No 1	44
32	Electrolyte Excursion Data, Two-Cell Plaque No 3, Cell No 2	45
33	Performance History, Two-Cell Plaque No 3	46
34	Electrolyte Excursion Data, Two-Cell Plaque No. 3, Cell No. 1	47

ILLUSTRATIONS (Cont'd)

No	Title	Page
35	Performance History, Two-Cell Plaque No 3	47
36	Electrolyte Excursion Data, Two-Cell Plaque No. 3	48
37	Electrolyte Excursion Data, Two-Cell Plaque No 3	49.
A-1-A-5	Pressure/Saturation Summary	
B-1	Water Expulsion Characteristics of Nickel-Plated Polysulfone Electrolyte Reservoir Plate	

TABLES

No.	Title	Page
I	Design Details of Cells Tested	6
II	Single Cell Test Summary	7
III	Single Cell No. 42 Performance Summary	10
IV	Single Cell No. 44 Performance Summary	14
V	Two-Cell Plaque Designs Tested	30
VI	Two-Cell Plaque No 2 Performance Summary	38
VII	Two Cell Plaque No 3 Performance Summary	42
B-1	Measured ETU	
B-2	Porosity Results	

ABSTRACT

An experimental program was conducted continuing the development effort to improve the weight, life, and performance characteristics of hydrogen-oxygen alkaline fuel cells for advanced power systems. These advanced technology cells operate with passive water removal which contributes to a lower system weight and extended operating life.

During the program covered by this report, endurance evaluation of two single cells and two, two-cell plaques initiated under contract NAS3-15339 was continued. In addition three new test articles were fabricated and tested. A single cell completed 7038 hours of endurance testing. This cell incorporated a Fybex matrix, hybrid-frame, PPF anode, and a 90 Au/10 Pt cathode. This configuration was developed under this program to extend cell life. Two-cell plaques with dedicated flow fields and manifolds for all fluids did not exhibit the cell-to-cell electrolyte transfer that limited the operating life of earlier multicell plaques.

Another electrolyte transfer phenomenon between cell and passive water removal unit was identified and found to be the result of a wettable hydrogen flow field. Substitution of a non-wettable flow field appeared to prevent this electrolyte transfer. At the conclusion of this program, 4912 hours of two-cell plaque testing and 12,668 hours of single cell testing were completed.

I. SUMMARY

This document reports the activity and results of a long range research program to improve the life, weight and performance of alkaline fuel cells. The advanced technology Fuel Cells are being developed to meet requirements of future NASA missions. These cells have a specific weight of 4 lbs/kW which is half the weight incorporated in PSD's PC17 Space Shuttle Fuel Cell Powerplant.

The advanced technology cells operate with passive water removal which offers a potential for additional powerplant weight savings and extended life. Passive water removal eliminates the requirement for a hydrogen circulating pump and dynamic water separator.

Objectives

There were two objectives of the work performed under this contract. The first objective was to continue the evaluation of advanced technology fuel cell endurance initiated under the previous contract NAS3-15339. A second objective was to evaluate a design change to eliminate electrolyte transfer between cells.

Scope

Two single cells and two, two-cell-plaques which were fabricated and tested under contract NAS3-15339 and a single cell fabricated under a PSD independent research and development program were continued on test.

In addition a single cell and one additional two-cell plaque were fabricated and tested.

Results and Conclusions

A total of 12,688 hours of single cell testing and 4,912 hours of two-cell plaque testing was completed. Single cell testing indicated the possibility of extended operating life with the elimination of silicon from the cell.

The two cell plaque testing demonstrated that dedicated manifolding along with complete isolation of each cell prevented electrolyte transfer from cell-to-cell in two-cell plaques.

The apparent transfer of electrolyte from the cell to passive water removal assembly was determined to be due to the introduction of a wettable material to form the hydrogen flow field between the cell and product water removal assembly. When this field was replaced with a molded polypropylene screen no evidence of electrolyte transfer was observed in over 700 hours of testing. In addition a cell with a molded Teflon screen as the hydrogen flow field completed over 300 hours of endurance with no evidence of electrolyte transfer. This cell was continued on endurance under contract NAS3-20042 and plans are to verify the solution in a two-cell plaque under that contract.

Teardown inspection of a two-cell plaque revealed inconsistent plating of the porous polysulfone electrolyte reservoir plate and a manufacturing investigation resulted in improved plating procedures. These procedures provide consistent plating and improved performance of the electrolyte reservoir plate

An advanced fuel cell design has been demonstrated which has a specific weight one-half the weight of the cell design presently utilized in the Space Shuttle Orbiter Fuel Cell Powerplant.

Each of the tasks and results achieved are reported in detail in the following sections.

II INTRODUCTION

Background

Power Systems Division has been conducting a series of contracts under the direction of the Lewis Research Center of NASA. These contracts are concerned with improving fuel cell technology for future space power applications.

Work accomplished under previous contracts has been reported in References 1, 2, 3 and 4. The final contract in this program is NAS3-20042

Prior work identified and demonstrated cell designs with reduced corrosion rate and extended endurance

A cell structure was developed using a combination of fiberglass/epoxy and fiberglass/polysulfone laminations. This structure demonstrated reduced corrosion rates so that the build up of carbonates in the potassium hydroxide electrolyte due to corrosion of the cell structure was reduced by a factor of 3

A porous polysulfone electrolyte reservoir plate (ERP) has been demonstrated which replaces the sintered nickel ERP in the space powerplants and is a major factor in reducing cell specific weight from 8 lbs/KW to 4 lbs/KW

A passive water removal assembly has been demonstrated which eliminates the requirement for rotating machinery to remove the water which is generated during cell operation. This results in powerplant designs with reduced weight and the potential for higher reliability and extended endurance

A method of edge current collection has been demonstrated which allows the introduction of light weight plastic materials between cell assemblies in place of metal elements which are required now.

Cell designs have been demonstrated with areas of $1/10$ and $1/4$ ft² compared with $1/2$ ft² which is incorporated in the Space Shuttle Orbiter powerplant. This permits a better match for low powered applications for fuel cells. A multi-cell plaque design has been demonstrated with up to six cells assembled in a coplaner array within a common structural frame

Polybenzimidazole and potassium titanate have been identified as materials for electrolyte matrices with the potential to extend cell life, and an advanced structural resin with low corrosion rate and the ability to operate at elevated temperatures has been identified

At the conclusion of the preceding contract, NAS3-15339, two single cells and two 2-cell plaques were undergoing endurance testing

Transfer of electrolyte between cells within a common plaque has been observed and is a problem which limits the operating life of the plaque concept

Related Work

Work is underway at Power Systems Division on a contract with Marshall Space Flight Center to incorporate many of the technology advances demonstrated under the current Lewis contract in the design of a small light weight space powerplant with a nominal power rating of about 2 KW and a specific weight of 17.5 lbs/KW. The work under the Marshall contract will culminate in a demonstration of a 28V power section using a cell with an area of 1/4 ft² and incorporating passive water removal assemblies.

Scope

The scope of the current contract includes continued testing of two single cells and two, two-cell plaques which were fabricated and placed on test during contract NAS3-15339 and the fabrication and test of two additional single cells and a two-cell plaque.

Relevance and Significance of the Work Reported

The performance and endurance of lightweight cell assemblies with a 50 percent reduction in weight compared with cells in current space powerplants has been demonstrated. These cells operate with passive water removal assemblies which permit a powerplant design with reduced weight and extended endurance.

The use of independent gas manifolds as opposed to common gas manifolds has been shown to eliminate cell-to-cell electrolyte transfer in multi-cell plaques.

Transfer of electrolyte from the cell to passive water removal assembly has been observed. This appears to be due to the presence of wettable structures between the cell and the passive water removal assembly. Additional testing is required to confirm this hypothesis and to correct the problem which results in limited operating life of cells with passive water removal assemblies.

Test Conditions

Tests are conducted in test stands originally built for the Apollo fuel cell program in 1963, modified to meet the requirements of the current cells.

Operating pressure in the cells is approximately 1 atmosphere at a temperature of 180°F. A vacuum of 21.8 in Mercury is maintained adjacent of the passive water removal assemblies to achieve water removal.

III SINGLE CELL FABRICATION AND TESTING

A Single Cell Design

This section describes the design of the single cell test hardware and the single cell design configurations evaluated in the program. The single cell test unit used in performance and endurance testing incorporate the following novel features

- Strip cell - 12.0 x 1.375 inches (30.5 x 3.49 cm) cell area
- Edge current collection
- Passive Water Removal
- Improved Compatibility frame
- Minimum thickness flow fields and component parts

The cell assembly consists of two sections the unitized electrode assembly (UEA) and a passive water removal (PWR) unit. These two components can be either bonded together or mated with an elastomer gasket between them to effect the required seal.

The cell test fixtures used during the program were rigid ½ inch (1.27 cm) stainless steel plates with provision for sealing and fluid connections. Some of the features of the test fixture include

- Flow field inserts for interchange of field patterns
- O-ring sealing for easy assembly of unitized parts.
- Isothermal operation
- Passive heat rejection for test simplicity
- Nickel plated to avoid corrosion

The cell configurations tested during the program are described in detail in Table I.

TABLE I
DESIGN DETAILS OF CELLS TESTED

<u>Cell Number</u>	<u>NASA Design Number</u>	<u>UEA Description</u>	<u>PWR Description</u>	<u>Oxygen Field</u>	<u>Hydrogen Field</u>
*42	12	Hybrid Polysulfone/ Epoxy-Glass Fiber Prepreg PPF Anode 90Au-10Pt Cathode 30 mil (0 76 mm) Polysulfone ERP Fybex Matrix	Epoxy-Glass Fiber Frame, 22-mil (0 56-mm) Porous Polysulfone, 20 mil (0 51-mm) RAM Goretex Membrane	Machined Insert 15 mil (0 38 mm)	Polypropylene Screen 33 mil (0 84 mm)
*44	12	Same as 42	Same as 42 except 10 mil (0 25 mm) Matrix at 1323 load hours	Same as 42	Teflon Screen 28 mil (0 71 mm)
45	R&T	Epoxy-Glass Fiber Prepreg PPF Anode 90Au-10Pt Cathode 30-mil (0 76 mm) Polysulfone ERP 10-mil RAM	Epoxy-Glass Fiber Frame, 22-mil (0 56 mm) Porous Polysulfone, 20 mil (0 51-mm) RAM Goretex Membrane 10 mil RAM and 30-mil ERP @ LT-1273 Hrs	Electroformed 3 Mil Ni, 15 Mil Field Depth	50 mil Ni Kintex TFE Screen at LT = 1273 Hrs
46	R&T	Hybrid Polysulfone/ Epoxy-Glass Fiber Prepreg PPF Anode 90Au-10Pt Cathode 30 mil (0 76 mm) Polysulfone ERP 10-mil RAM (0 25mm)	Epoxy-Glass fiber Prepreg 10-mil RAM (0 25mm) 30-Mil Polysulfone (0 75 mm) ERP Goretex Membrane	Same as 42 Electroformed 3 mil Ni 15-mil Field Depth at LT = 791 Hrs	Same as 42 TFE Screen @ LT = 1492 Hrs

R&T-PSD Research and Technology Program

LT -- Load Time

*Begun under Contract NAS3-15339

B. Single Cell Test Results

This section reviews each of the cell tests conducted during this program. The results of these tests are summarized in Table II

TABLE II
SINGLE CELL TEST SUMMARY

Cell No	Load Time (Hrs)	Performance** (Volts)			Initial IR (mv @ 100 ASF)**	Percent Conversion to K_2CO_3
		Initial	Peak	Final		
*42	7090	912	912	885	7.0	9.96% @ 342 hrs 33% @ 6516 hrs
*44	7513	910	910	825	9.0	16.0% @ 1323 hrs 42.5% @ 4712 hrs
45	2430	932	932	894	11.0	—
46	1842	922	922	912	8.8	—

*Begun under Contract NAS3-15339

**100 ASF (107.6 ma/cm²)

Cell Nos. 42 and 44

These cells were fabricated with hybrid polysulfone/epoxy-glass fiber frames with standard PPF anodes, 90Au-10Pt cathodes, polysulfone ERP's and Fybex matrices. The objective of the tests was to evaluate the endurance characteristics of Fybex-matrix cells. Because of its non-corroding characteristics, the Fybex matrix was expected to improve the endurance characteristics of these cells. Silicates in asbestos were found to produce, over very long operating periods, silicon containing deposits on the anode which caused anode flooding and performance degradation.

Cell No. 42

During the previous contract (ref. 1) cell No. 42 accumulated 4405 hours at a current density of 100 ASF (107.6 ma/cm²), 180°F (82.2°C) cell temperature, and 16 psia (11.03 N/cm²) reactant pressure. The cell during this program accumulated an additional 2685 hours for a total load time on the cell of 7090 hours. The complete performance history of the cell is shown in Figure 1.

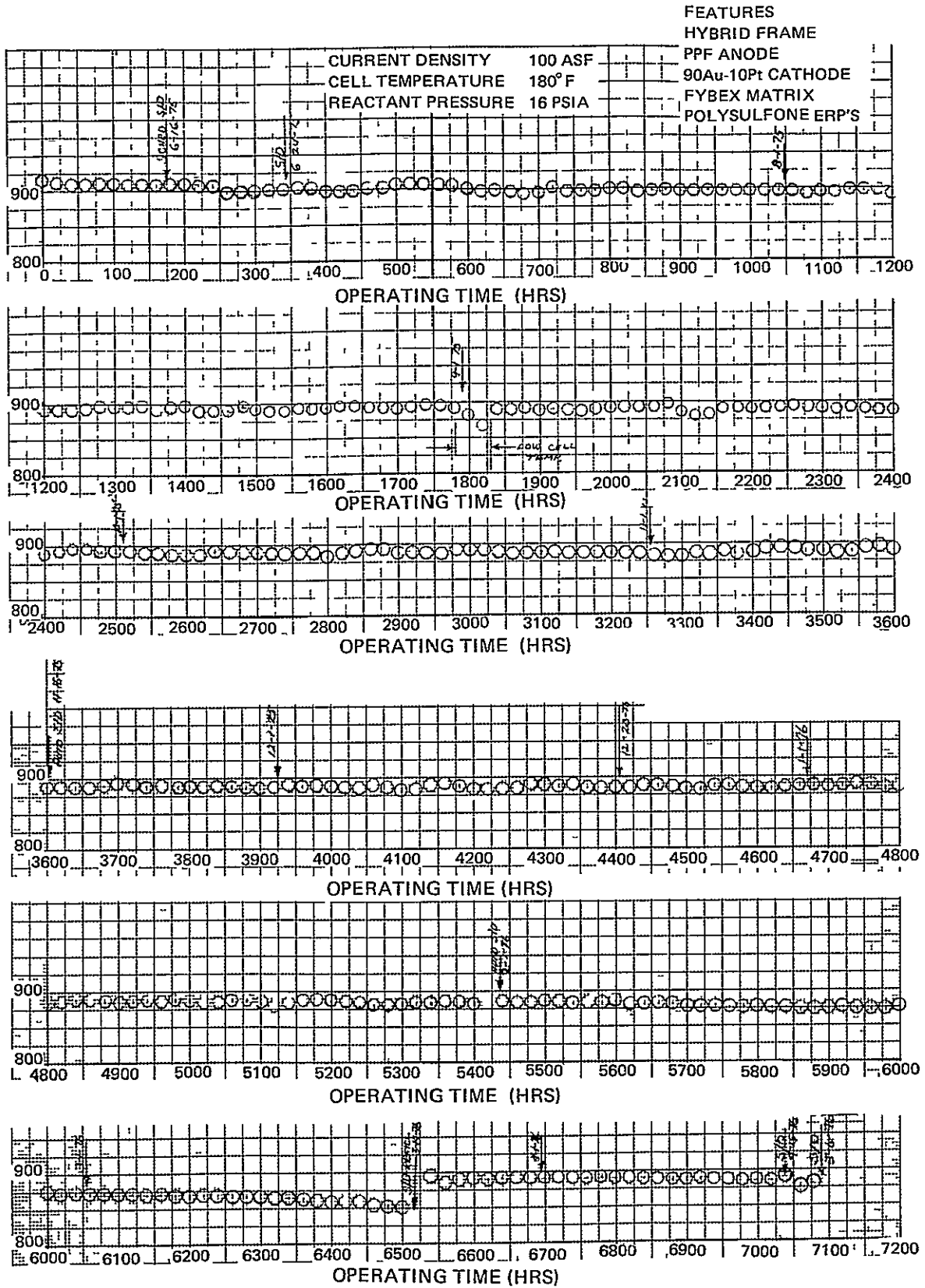


Figure 1 – Performance History, Single Cell No 42

The final performance of the cell was 0.885 volts which is only a 27mV reduction in voltage over the course of the endurance test. This performance history represents the best characteristics of any cell in NASA-LeRC series. The stabilization of anode diffusion losses resulting from the absence of silicon in the matrix was the primary difference between cell No. 42 and other long term cells. The effect of a silicon free, Fyber matrix cell compared to a asbestos matrix cell in the reduction of anode diffusion losses with time is shown in Figure 2. The results of dilute oxygen diagnostic tests performed during the endurance test are summarized in Table III. A reduced open circuit voltage experienced at 5014 hours was identified as a slight internal cell short.

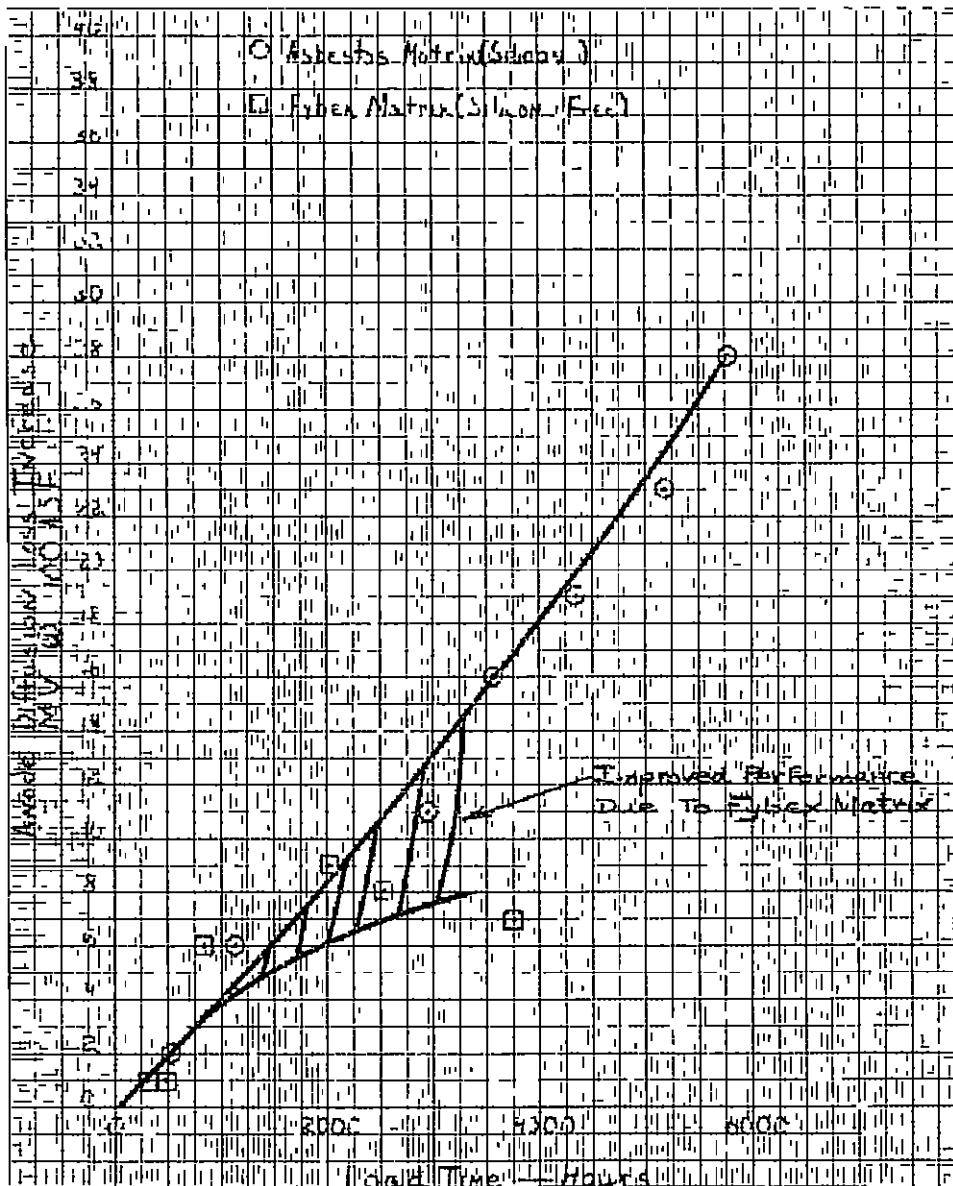


Figure 2 – Anode Diffusion Loss Comparison

NOT REPRODUCIBLE

TABLE III
SINGLE CELL NO 42 PERFORMANCE SUMMARY

Frame Hybrid Polysulfone Epoxy Glass Fiber
Cathode 90 Au 10 Pt
Anode PPF
ERP Polysulfone
Matrix Fybex

LOAD TIME (HRS)	PERFORMANCE			IR (mV)	ACTIVATION LOSS (mV)	DIFFUSION LOSS (100 ASF)		
	1 0 ASF	2 0 ASF	100 ASF*			TOTAL (mV)	ANODE (mV)	CATHODE (mV)
21	1 024	1 012	917	7	--	13	10	3
320	1 019	1 006	907	7.5	5	18	11	7
482	1 020	1 007	905	6.0	4	19	11	8
846	1 018	1 004	898	6.2	6	21	16	5
2018	1 017	1 003	894	6.0	7	25	19	6
2534	1 019	1 005	895	7.0	5	25	18	7
3757	1 019	1 006	896	7.0	5	27	17	10
5014	1 017	1 003	894	8.0	7	28	--	--

*Performance Corrected For Cell IR

Cell voltage response to changes in electrolyte concentration was evaluated at several times during the endurance test as shown in Figure 3. The cell voltage response up to 4348 hours was normal. However, by 5987 hours there was almost no increase in cell voltage as the electrolyte concentration was raised from 34 wt % KOH to 40 wt. % KOH. The reduction in voltage response can result from carbonation of the electrolyte.

At 6516 hours the cell was subjected to an electrolyte refill in order to identify the carbonate level. The analysis showed that 33 percent of the electrolyte was converted to carbonate which is consistent with past polysulfone/epoxy-glass fiber hybrid frame corrosion experience as shown in Figure 4. The stabilized performance following the refill was 0.890 volts at 100 ASF (107.6 ma/cm²) which represents a recovery to the 2500 hour level. The elimination of carbonates within the electrolyte would account for about 95 percent of the voltage improvement and the remainder would result from the flushing out of other contaminants.

An increase in the amount of internal shorting was identified at 6900 hours by continuing reduction of open circuit voltage. Endurance testing was discontinued at 7038 hours when symptoms of reactant gas crossover were experienced.

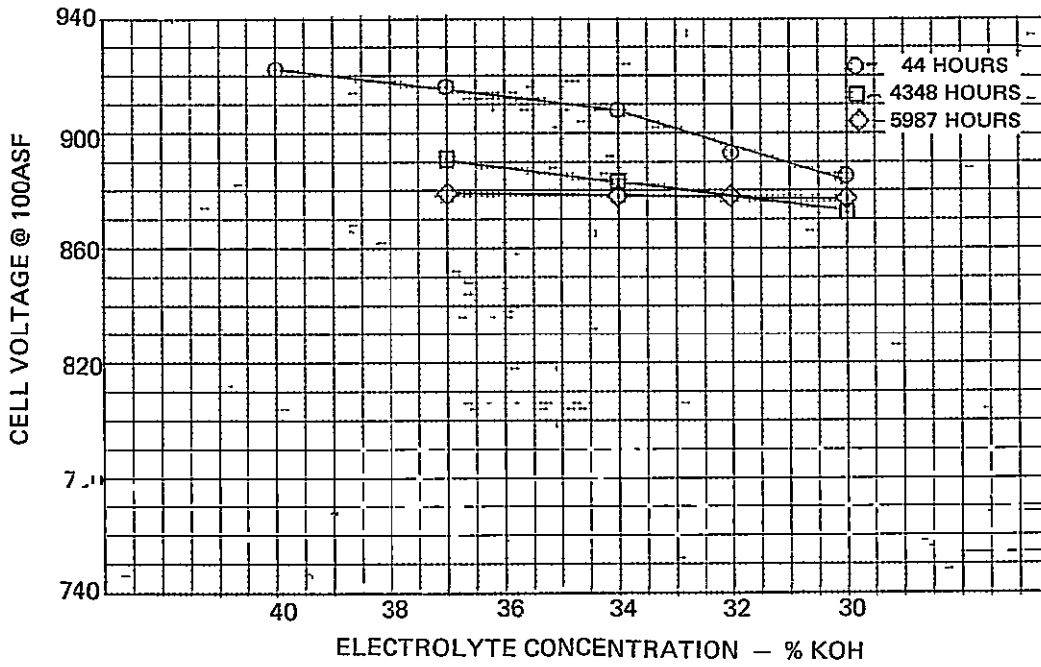


Figure 3 - Electrolyte Excursion Data, Single Cell No 42

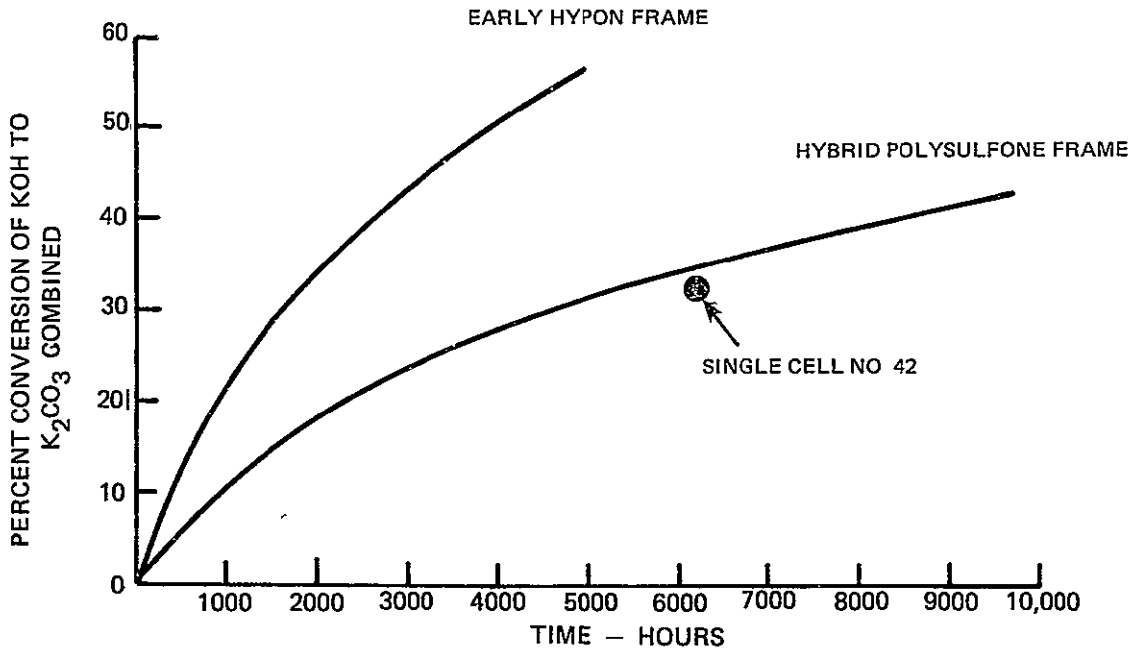


Figure 4 - Electrolyte Conversion to Carbonate, Single Cell No 42

Visual inspection of the cell after disassembly identified the location of the crossover site to be in the cell frame at the edge of the active area near the oxygen inlet. A repair was made by sealing the site and the cell was refilled with electrolyte. Following return to endurance conditions there continued to be evidence of reactant crossover. All further endurance operation was stopped at 7090 hours.

Teardown inspection of the cell indicated that all parts were in good condition except in the area of the crossover. Samples from the anode were half-cell tested and showed only a 12 mV at 100 ASF (107.6 ma/cm²) loss even though the sample appeared wettable. Operating the anode sample as a cathode revealed a 50 percent reduction in catalyst activity. A hydrogen fluoride leach of the electrode to remove contaminants restored the performance to nearly that of a new anode. A portion of the anode was micro-sectioned. Microscopic examination showed that some Fybex particles may have penetrated into the interior of the catalyst layer possibly contributing to some anode flooding during the endurance test. Although the anode did appear to have a propensity to flood, the total anode polarization increase after 7000 hours was consistent with past NASA-Lewis cell experience. In addition, the restoration of anode performance with the hydrogen fluoride leach was indication that some contamination of the anode had occurred.

Cell No. 44

Cell No. 44 was constructed to the same configuration as Cell No. 42 except the cell's matrix was fabricated without Triton wetting agent to eliminate any possibility of electrode poisoning from that source. This cell during the previous contract (ref. 1) accumulated 1719 hours at current density of 100 ASF (107.6 ma/cm²), 180°F (82.2°C) cell temperature and 16 psia (11.03 N/cm²) reactant pressure. The cell during this program accumulated an additional 5794 hours for a total load time of 7513 hours. The complete performance history is shown in Figure 5 and a compilation of accountable losses is shown in Table IV.

TABLE IV
SINGLE CELL NO 44 PERFORMANCE SUMMARY

Frame Hybrid Polysulfone.Epoxy Glass Fiber
Cathode 90 Au 10 Pt
Anode PPF
ERP Polysulfone
Matrix Fybex

LOAD TIME (HRS)	PERFORMANCE			IR (mV)	ACTIVATION LOSS (mV)	DIFFUSION LOSS (100 ASF)			COMMENTS
	1 0 ASF	2 0 ASF	100 ASF*			TOTAL (mV)	ANODE (mV)	CATHODE (mV)	
21	1 026	1 013	920	9	—	20	13	7	
515	1 017	1 004	907	10	9	23	17	6	
1345	1 026	1 013	918	9	—	19	12	7	PWR REPLACED
2920	1 021	1 006	893	11	5	37	22	15	
4765	1 011	996	868	11	15	51	39	12	AFTER REFILL
5708			856	11	—	—	—	—	

*Performance Corrected For Cell IR

The rate of cell performance fall off remained relatively constant until the cell was shutdown at 4712 hours for an electrolyte refill in order to determine electrolyte carbonate content. Analysis of the electrolyte identified that 42.5 percent of the KOH was converted to K_2CO_3 . Figure 6 shows that this conversion is significantly higher than typically experienced with hybrid frame UEA cells. Subsequently, the silicone rubber gasket used to seal the PWR to the UEA was found to be a principal source for the high carbonate levels. Evaluation of cell performance response to changes in electrolyte concentration shown in Figure 7 indicated a normal response. Dilute oxygen diagnostic data at 2920 hours revealed that the majority of the performance loss was in the electrode diffusion region. In addition this data indicated that there was no evidence of cell shorting or reactant crossover.

Upon resumption of the endurance program, 4712 hours, cell performance had improved 26 mV at 100 ASF (107.6 ma/cm^2). This performance recovery agrees closely with the predictions of performance improvement for the elimination of electrolyte carbonation. A reduced open circuit voltage during dilute oxygen diagnostic test at 5708 hours was identified as a small internal short. The increasing magnitude of the short forced termination of the endurance program at 7513 hours.

Teardown inspection identified white deposits at the oxygen inlet ports and some disintegration of the silicone rubber gasket along its inner diameter. Otherwise the cell appeared to be in good condition.

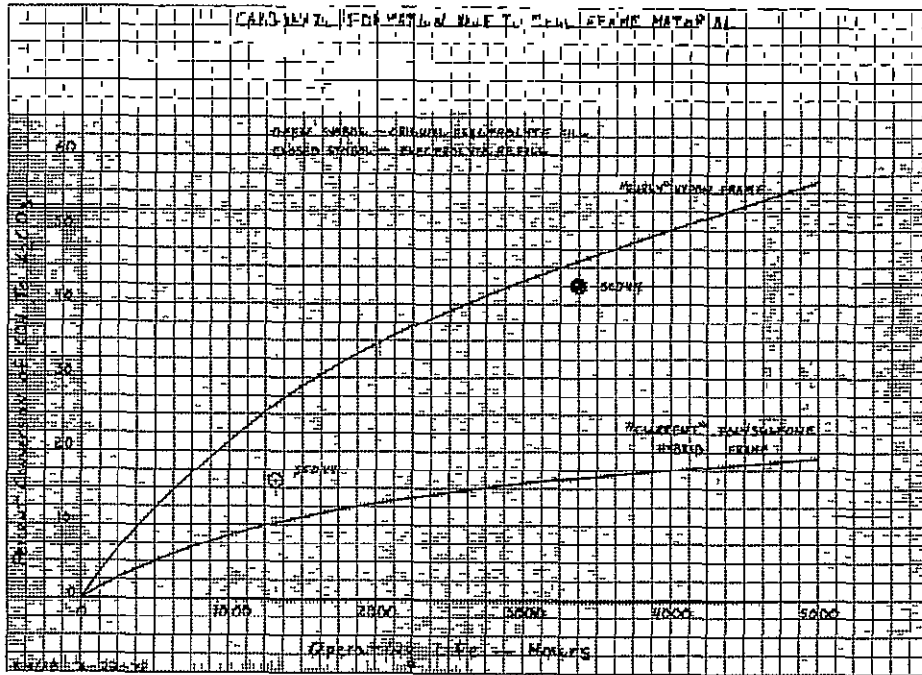


Figure 6 — Electrolyte Conversion to Carbonate, Single Cell No 44

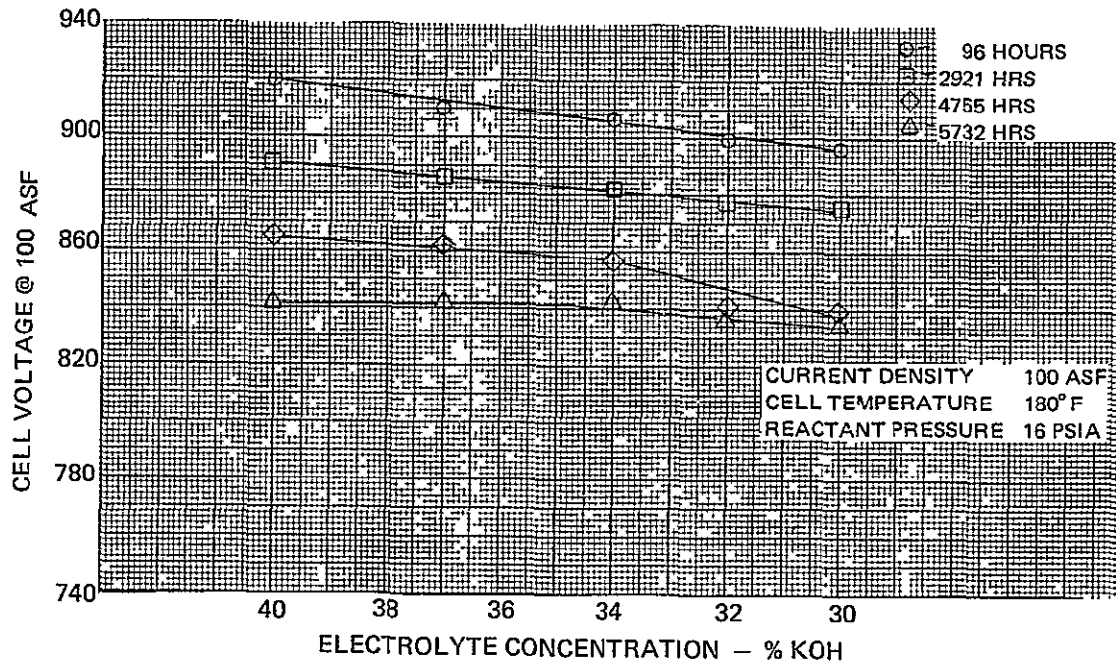


Figure 7 — Electrolyte Excursion Data, Single Cell No 44

While Cell No. 44 did not exhibit the long term stable performance characteristic of Cell No. 42, the primary reason appears to be the presence of the silicone rubber gasket. This gasket apparently not only contributed to an excessive carbonate level in the electrolyte but may have also led to premature flooding of the anode. The shorting that was experienced by both of these cells and two-cell plaque Nos. 1 and 2 has led to a design change in the hybrid cell configuration. It was found that strands of the electrode screens were shorting to each other through the polysulfone frame material adjacent to the matrix. To avoid this the electrode screens were cut back so that they do not extend beyond the edge of the matrix.

Cell No. 45

This cell was fabricated with a glass fiber epoxy frame, standard PPF anodes 90Au-10Pt cathode, polysulfone ERP's and 0.010 in. thick (0.025) asbestos matrix. The unique features were the reactant gas flow fields which consisted of an electroformed nickel oxygen field and a nickel Kintex hydrogen field. A cross section of the cell is shown in Figure 8. This cell was utilized initially for 91 hours in a PSD sponsored helium diluted reactant test. The cell was refilled with electrolyte prior to initiation of the endurance test because the cell had been stored in an uncontrolled environment. The test objective for the cell was to investigate the cell to PWR electrolyte transfer phenomenon discussed in Appendix A. During this program the cell accumulated 2325 hours at a current density of 100 ASF (107.6 ma/cm^2), 180°F (82°C) cell temperature and a reactant pressure of 16 psia (11.03 N/cm^2). The performance history of the cell is shown in Figure 9.

During the initial 810 hours of operation the performance level and cell voltage response to an electrolyte concentration change was investigated.

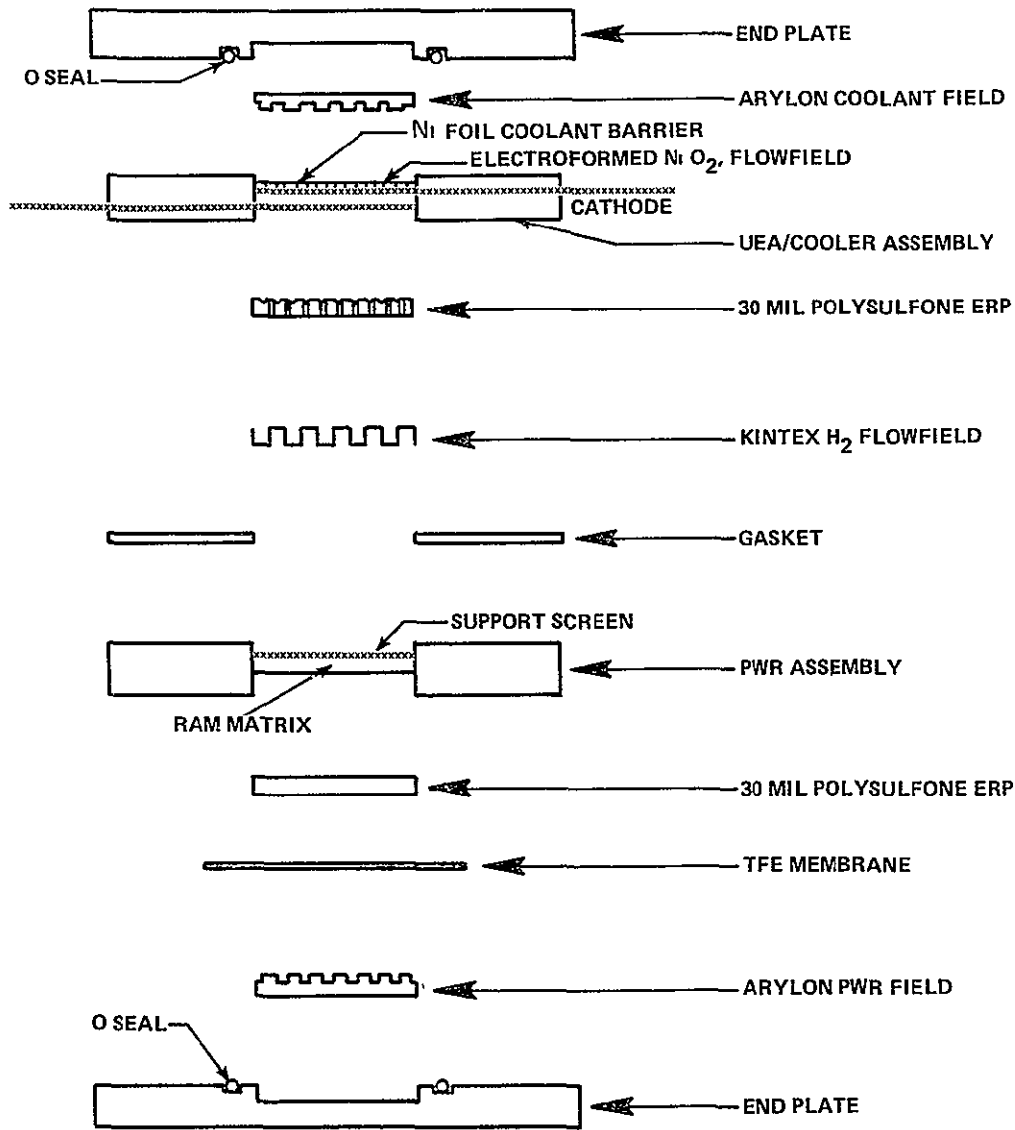


Figure 8 – Cross Section, Single Cell No 45

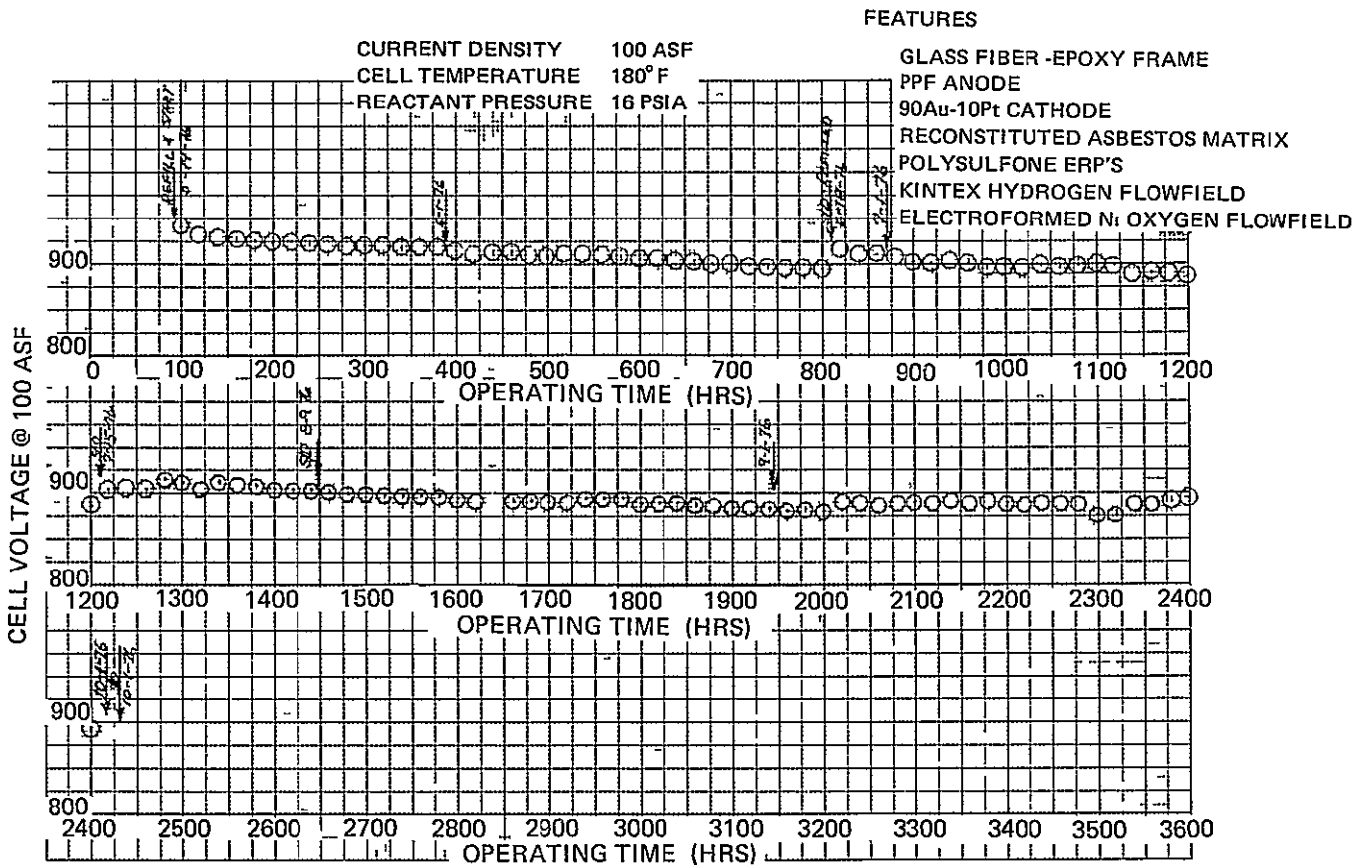


Figure 9 – Performance History, Single Cell No 45

The performance increase at 112 load hours as the cell electrolyte concentration was raised to 40 wt. % from 34 wt. % KOH as shown in Figure 10 represents normal cell response. The continual decrease in performance response over the same concentration range as experienced at 496 hours is an indication of a reduction in cell electrolyte inventory. Gradual performance fall-off and continued indication of reduced electrolyte inventory required the interruption of test at 808 hours for an electrolyte refill. This performance characteristic was the same as exhibited on the two-cell plaque configuration which suggested that the electrolyte transfer phenomenon was related to the cell assembly and not the higher voltages of the two cell plaque.

Visual inspection of cell components at shutdown identified some deterioration of the silicone rubber gasket between the UEA and PWR unit. This gasket was replaced with an ethylene propylene rubber (EPR) seal before the electrolyte refill. In addition, the original polysulfone ERP was replaced with an ERP plated by the new process to ensure good wettability (Appendix B). Prior to restart, a hydrogen preheater was installed in the stand to minimize effects of any possible cell cooling and inlet flooding.

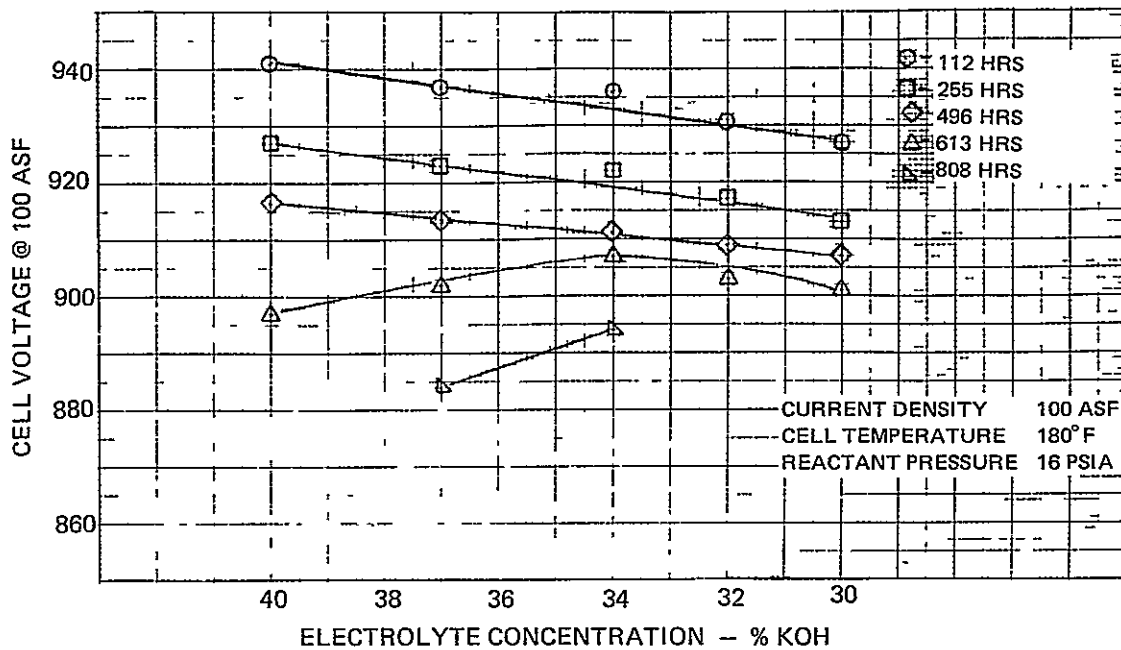


Figure 10 – Electrolyte Excursion Data, Single Cell No 45

Upon resumption of endurance operation the performance level and voltage response to electrolyte concentration was similar to initial test results. At 1185 hours, 376 hours since the electrolyte refill, there was an indication of a performance drop as the operating electrolyte concentration was increased from 34 wt. % to 40 wt. % KOH. Results from the electrolyte excursion testing are shown in Figure 11. This consistency between the first and second sets of test data indicated that the reduction in performance response to dry side electrolyte concentration (40% wt. KOH) operation was not associated with either the silicone rubber gasket corrosion or the polysulfone ERP. Prior to ending the endurance test nitrogen was introduced into both reactant cavities to assist in identifying the dry side electrolyte concentration limit of the UEA and PWR. The objective of this special test was to determine if the electrolyte from the UEA was being transferred to the PWR unit. Calculations had shown that if the quantity of electrolyte lost from the UEA to give the performance response to dry side electrolyte concentration operation shown at 1185 hours had transferred to the PWR unit, the PWR unit would not empty and show crossover at 55 percent concentration instead of the normal 42 percent. This was confirmed since the PWR unit showed crossover symptoms at 54 percent.

ORIGINAL ...
 OF POOR QUALITY

**ORIGINAL PAGE IS
OF POOR QUALITY**

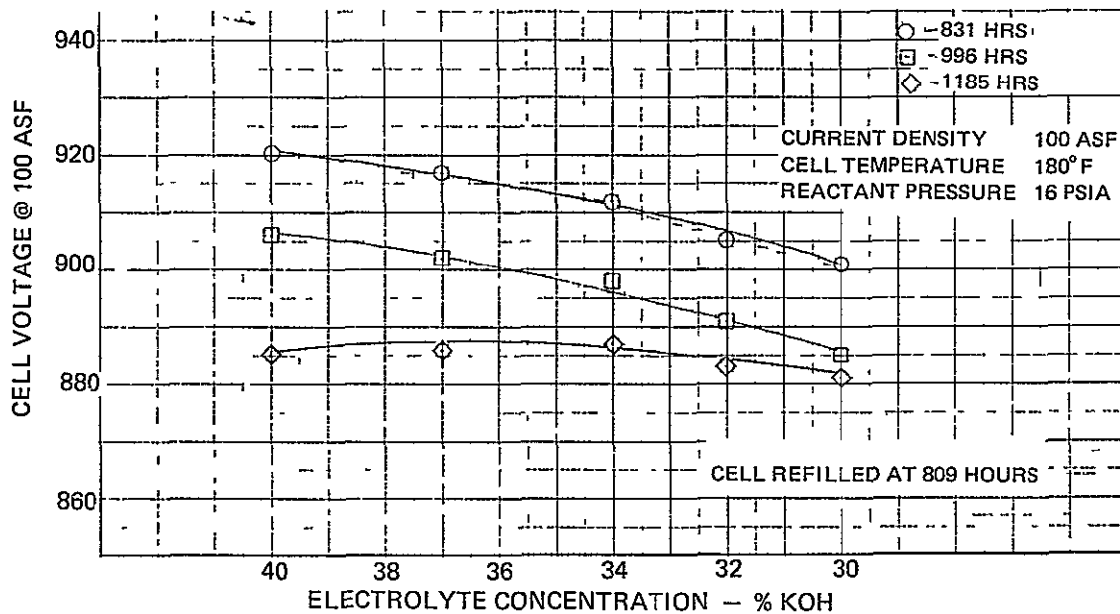


Figure 11 – Electrolyte Excursion Data, Single Cell No 45

Upon completion of the special test, the cell was subjected to an electrolyte refill. The refill at 1273 hours was necessary because of possible expulsion of KOH from the UEA and PWR during the testing. In order to retard the flow of electrolyte from the UEA to the PWR unit upon continuation of the endurance test, a non-wettable Teflon screen hydrogen flow field was installed to replace the nickel Kintex field. The Teflon screen flow field had been used previously in NASA-Lewis single cells Nos. 43 and 44 (ref 1) which did not exhibit the performance droop as the electrolyte concentration was increased.

The performance characteristics upon return to endurance conditions were different from previous experience. The major difference was that the performance drop at elevated electrolyte concentration previously evident at around 350 hours was not experienced until over 600 hours after the electrolyte refill (Figure 12) This improvement in long term dry side operating capability was very encouraging.

The endurance test was interrupted at 2005 hours in order to disassemble the unit for inspection. The hydrogen flow field was removed and compared with a new Teflon screen to establish relative wettability. There was no difference identified. Both screens appeared non-wettable. The cause of the continued electrolyte transfer is not fully understood. However, there exists the possibility that excess electrolyte from a refill could have established electrolyte paths between the UEA and PWR unit which renders the non-wettable Teflon screen ineffective.

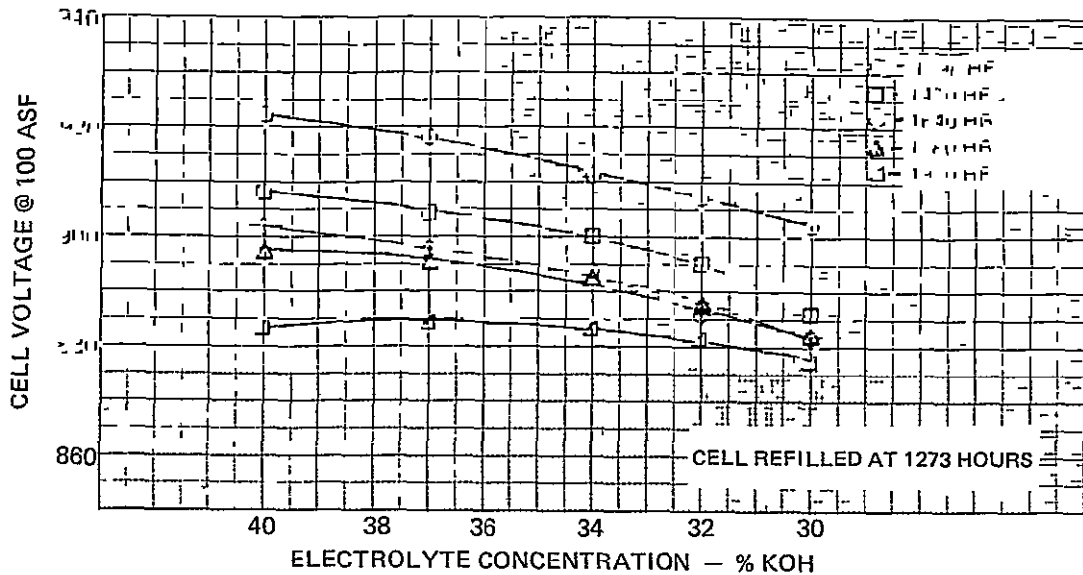


Figure 12 – Electrolyte Excursion Data, Single Cell No 45

In rebuilding the cell a porous Teflon membrane was installed between the anode ERP and the hydrogen flow field. This membrane was identical to the one in the PWR unit which prevents electrolyte loss into the product water cavity. Utilizing this membrane any electrolyte transfer from the UEA to PWR Unit should be eliminated. Upon resumption of the endurance test the cell performance response to electrolyte concentration variation as shown in Figure 13 was normal.

However, around 2364 hours evidence of reactant gas crossover was observed and the endurance test was stopped. Teardown inspection of the cell identified the crossover site to be in the frame at the oxygen inlet port. Slight frame corrosion was visible at the site, but a lack of resin or possible imperfections could not be identified as the cause of the crossover. There were no holes or defects found in the Teflon membrane between the UEA and PWR unit. Unfortunately, because of the crossover no conclusion relating to electrolyte transfer could be established.

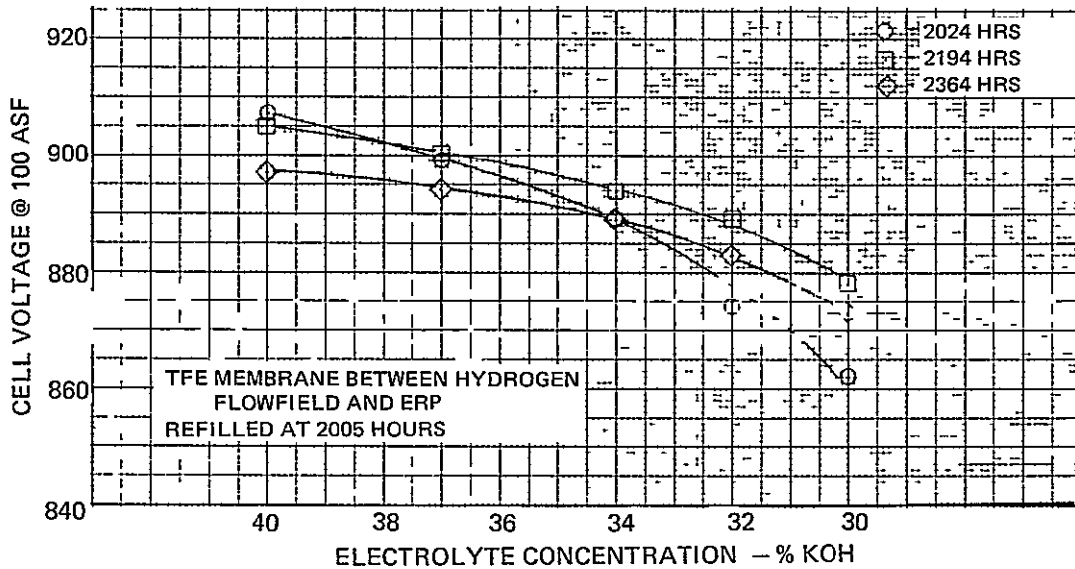


Figure 13 — Electrolyte Excursion Data, Single Cell No. 45

Single Cell No. 46

This cell was fabricated with hybrid polysulfone/epoxy-glass-fiber frame with standard PPF anode, 90 Au-10Pt cathode, 0.030 inch (0.076 cm) thick polysulfone ERP, and a 0.010 inch (0.025 cm) thick asbestos matrix. The hydrogen flow field was a 0.030 inch (0.076 cm) thick polypropylene screen and oxygen flow field was a machined, gold-plated nickel insert in the cathode end plate. A gasket was used in the hydrogen flow field and "O"-ring seals were used in both the PWR and oxygen flow fields. A cross-section of this cell is shown in Figure 14. Both the polypropylene screen hydrogen field and the nickel insert oxygen field were run successfully in previous NASA-Lewis cells.

This configuration represented an attempt to separate any fundamental cell manufacturing problems which could be causing electrolyte transfer from those encumbered by design changes inherent to the two-cell plaque.

Symptoms of electrolyte transfer had been observed in both single cell and two-cell plaque configurations. Each type of cell however had certain identical components and was subject to some of the same manufacturing procedures.

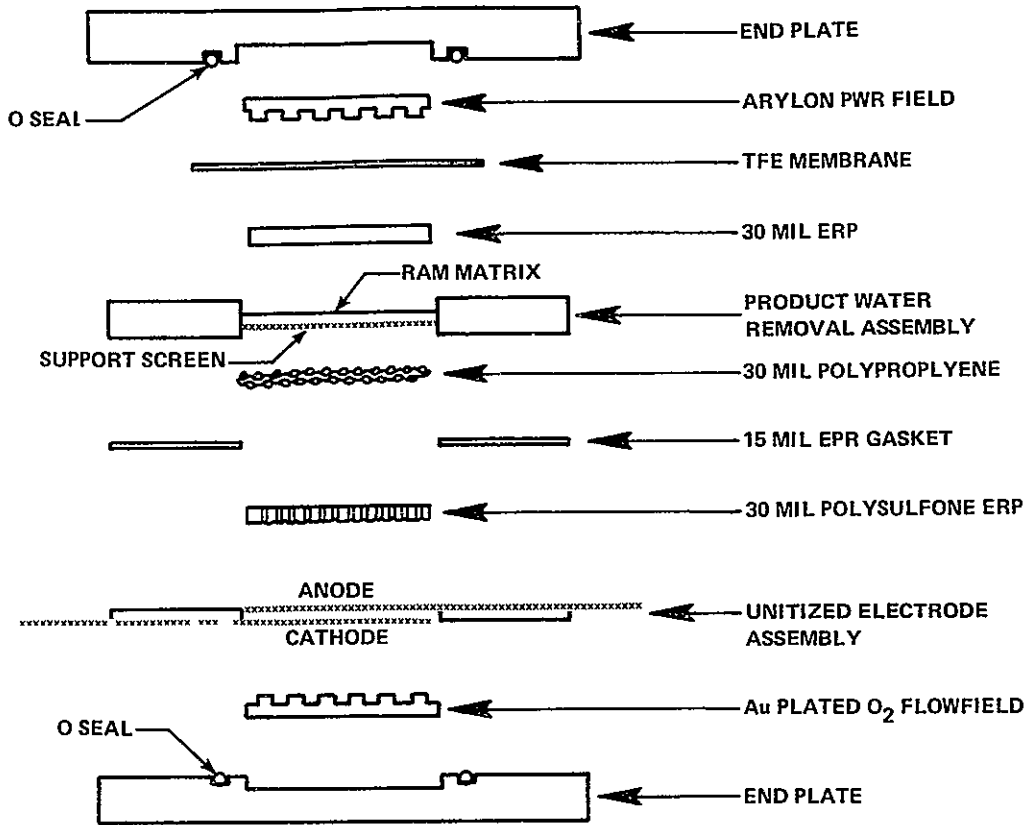


Figure 14 – Cross Section, Single Cell No 46

During this program the cell accumulated 1850 hours at 100 ASF (107.6 ma/cm²), 180°F (82.2°C) cell temperature and 16 psia (11.03 N/cm²) reactant pressure. The cell performance history is shown in Figure 15. In the first 790 hours of operation there was no evidence of a performance drop with increasing electrolyte concentration (Figure 16). Furthermore in the initial 1000 hour only 22 mV voltage degradation occurred compared to over 80 mV on cells which had symptoms of a reduction in cell electrolyte inventory. These normal performance characteristics suggest that inadvertent or unidentified changes in cell manufacturing procedures were not the cause of the cell electrolyte inventory reduction.

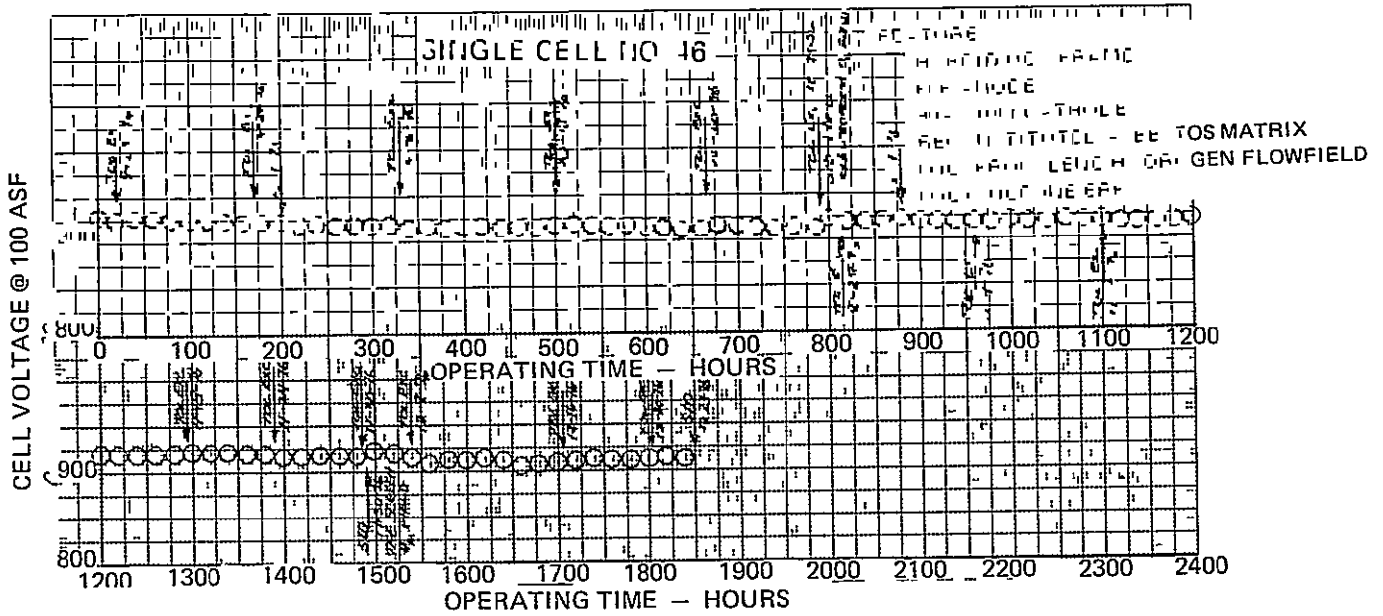


Figure 15 – Performance History, Single Cell No 46

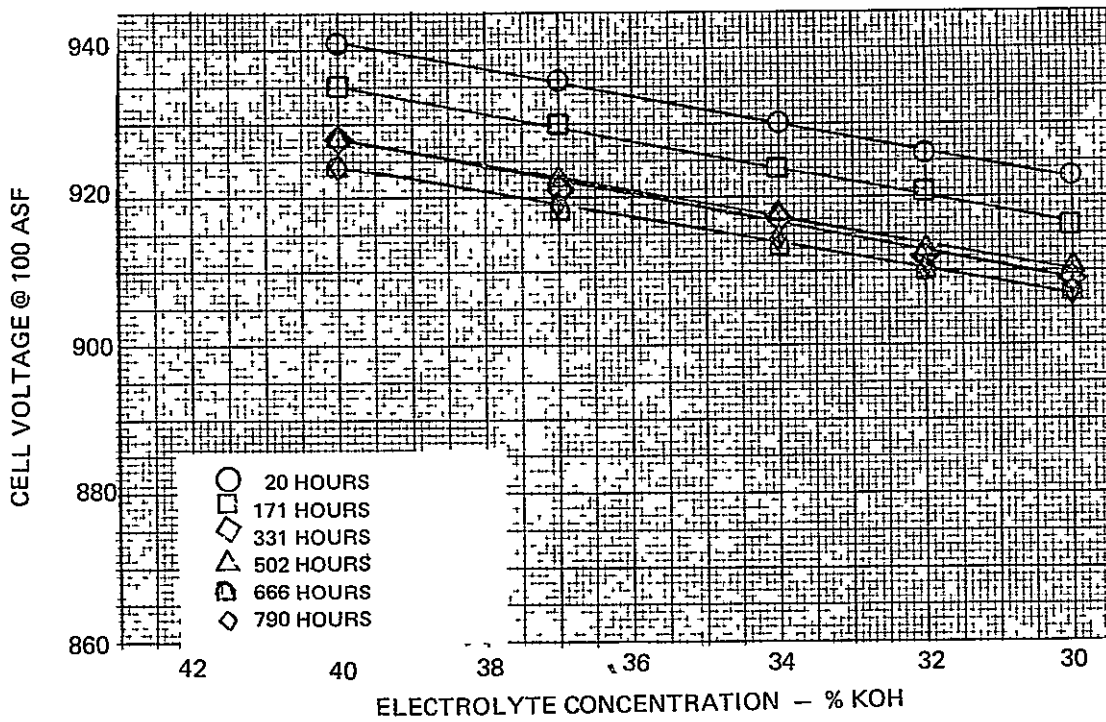


Figure 16 – Electrolyte Excursion Data, Single Cell No 46

At 791 hours the cell was rebuilt with an electroformed-nickel oxygen flow field in place of the machined nickel insert. The electroformed oxygen flow field was a component common to all cells that had shown a performance droop with time at increased electrolyte concentrations during endurance testing. In order to assure the correct distribution of electrolyte between the UEA and PWR unit, the cell was subjected to a electrolyte refill before continuing the endurance test. Electrolyte excursion data Figure 17, obtained periodically during the endurance program showed no change in performance characteristics at elevated electrolyte concentration in 695 hours. These test results indicated that the electroformed-nickel oxygen field was not responsible for the performance droop at elevated electrolyte concentrations, surmised to be a reduction in cell electrolyte inventory

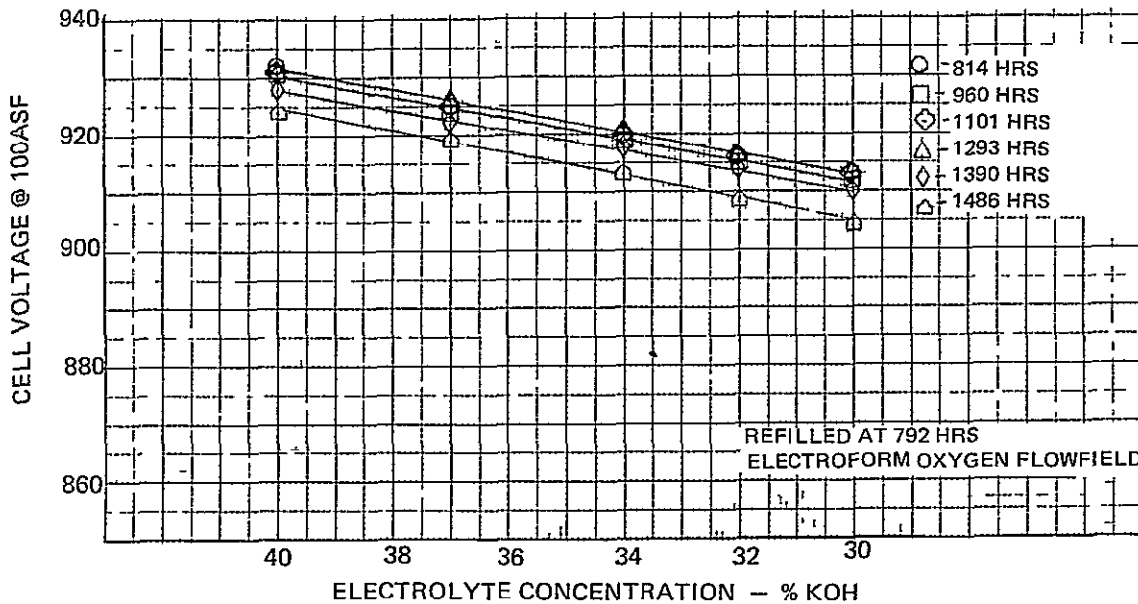


Figure 17 – Electrolyte Excursion Data, Single Cell No 46

The endurance program was interrupted at 1492 hours to install a non-wettable Teflon screen as the hydrogen flow field. Various diagnostic tests conducted on single cells and two-cell plaques have indicated that the reduction in dry-side electrolyte concentration operating capability with time appears to be due to a continuing reduction in cell electrolyte inventory from a transfer of cell electrolyte to the PWR unit. The base cell electrolyte loss model presented in Appendix A indicated that the normal pressure difference across the PWR unit acted as the driving force to move electrolyte from the UEA across the wettable nickel flow field to the PWR unit. Normal operation with passive water removal sets up a pressure differential to remove product water. The Teflon screen would effectively break any electrolyte paths across the hydrogen cavity. A

Teflon field was utilized in NASA-Lewis single cells 43, 44, and 45, as well as in Two-Cell Plaque No. 1. There was no evidence of a reduction in dry-side electrolyte concentration operating capability during endurance testing of cells 43, and 44. A reduction in the dry-side electrolyte operating concentration of cells in two-cell plaque No. 1 was traced to a poor plating quality of the ERP. Single cell No. 45 exhibited some loss in dry-side capability with time, however, the cell had excess electrolyte introduced during a refill, and possibly the residual electrolyte established a path between the UEA and PWR.

A total of 358 hours were accumulated on the Teflon flow field by the end of the program. Electrolyte excursion data, Figure 18, obtained during this period showed no loss in dry-side electrolyte operating capability. This was encouraging but not conclusive since the phenomenon had normally occurred in the 300- to 600-hour range. Figure 17 shows that the cell voltage dropped off sharply at 30 percent KOH during the electrolyte excursion test of 1541 hours. This was due to a test operator error which allowed a drop in cell temperature which not only lowered performance but resulted in a lower electrolyte concentration.

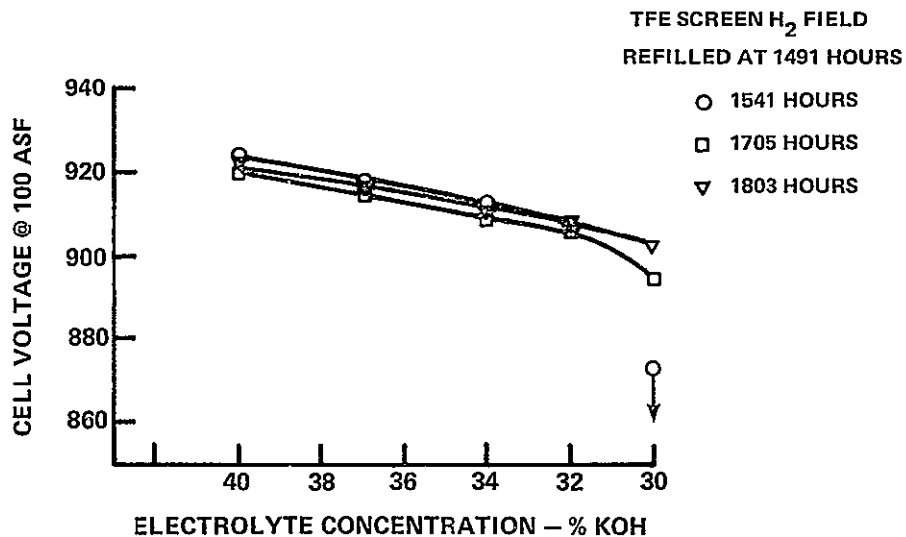


Figure 18 — Electrolyte Excursion Data, Single Cell No. 46

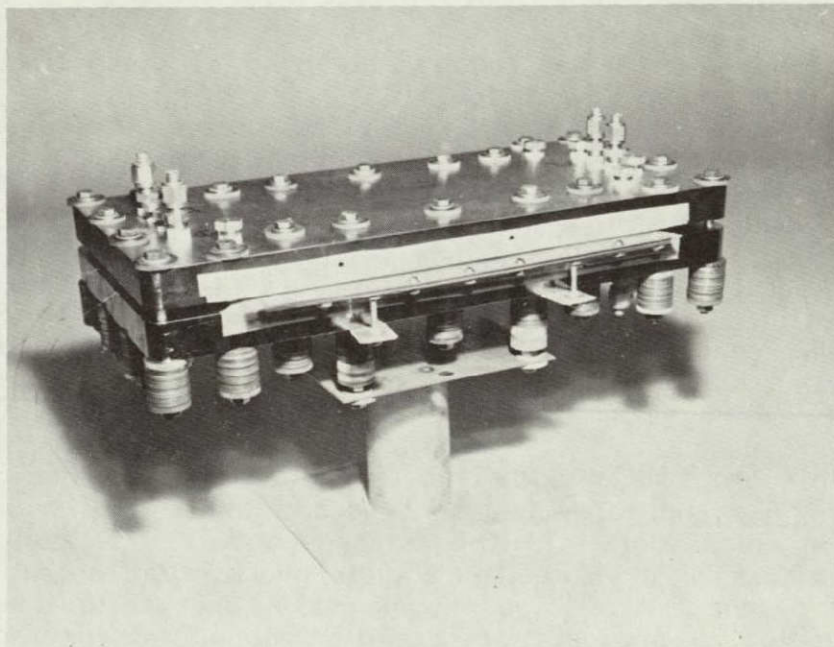
ORIGINAL PAGE IS
OF POOR QUALITY
PRECEDING PAGE BLANK NOT REPRODUCED

IV. TWO-CELL PLAQUE FABRICATION AND TESTING

A. Two-Cell Plaque Design

This section describes the design of the two-cell plaque hardware and the design configurations evaluated during the program. Each cell in the plaque incorporates the same design features as the single cells described in Section III B and is completed isolated from each other. As the cells are isolated, the plaque incorporates dedicated fluid manifolding for each cell. To insure the isolation of each cell, the plaque is assembled and bonded together as a complete unit. This was accomplished by bonding the center divider of each part together thereby forming a continuous barrier between cells. No elastomeric seals are present in the unit which might permit cell-to-cell leakage.

The plaque test fixtures used in the program consisted of 1.0 inch thick (2.54 cm) stainless steel end plates with provisions for sealing and fluid connections. The end plates included the same features and instrumentation as those of single cells. A two-cell plaque set up for endurance testing is shown in Figure 19.



(WCN-3656)

Figure 19 — Two Cell Plaque Test Setup

Preceding page blank

B. Two-Cell Plaque Test Results

The two-cell plaque configurations tested during the contract period are summarized in Table V.

TABLE V
TWO-CELL PLAQUE DESIGNS TESTED

<u>Plaque No.</u>	<u>NASA Design No.</u>	<u>UEA Description</u>	<u>PWR Description</u>	<u>Oxygen Field</u>	<u>Hydrogen Field</u>
1	1	Hybrid Polysulfone-Epoxy/Glass-Fiber Frame, Supported Catalyst Anode, 80Au-20Pt Cathode, 30-mil (0.76 mm) Polysulfone ERP	Epoxy/Glass-Fiber Frame, 20-mil (0.51 mm) RAM, 22-mil (0.56 mm) Polysulfone ERP Goretex Membrane	Electroformed 3-mil Ni 15-mil field depth	28-mil (0.71 mm) TFE Screen
2	2	Hybrid Polysulfone-Epoxy/Glass-Fiber Frame PPF Anode 90 Au-10Pt Cathode 30-mil (0.76 mm) Polysulfone ERP	Same as No. 1	Electroformed 3-mil Ni 15-mil field depth	38-mil (0.05 mm) Nickel Kintex
3	R/T	Epoxy/Glass-Fiber Frame PPF Anode, 90Au-10Pt Cathode, 22-Mil Ni ERP's	Epoxy/Glass-Fiber Frame, 20-mil RAM, 22-mil Polysulfone ERP Goretex Membrane	Electroformed 3-Mil Ni, 15-mil field depth	38-mil (0.05 mm) Nickel Kintex

Two-Cell Plaque No. 1

Two-Cell Plaque No. 1 was constructed using a hybrid frame UEA, supported catalyst anodes, and 80Au - 20Pt cathodes, and asbestos matrices. The hydrogen flow field was a Teflon screen and the oxygen flow field was electroformed-nickel. The ERP's in the UEA and PWR were nickel-plated polysulfone. This plaque was fabricated and accumulated 1644 hours of load time at a current density, of 100 ASF (107.6 ma/cm²), 180°F cell temperature and 16 psia reactant pressure during the previous program (ref 1). The complete performance history of the cell is shown in Figure 20. The first 1644 hours of endurance operation as reported in ref. 1 was characterized by a continuing loss of dry-side electrolyte concentration operating capability on cell No. 1 while the characteristics of cell no. 2 remained normal.

During this program an additional 897 hours of endurance operation was acquired. The endurance test was discontinued at 2531 hours to conduct a teardown inspection. In the final portion of the endurance test a continuing loss of dry-side electrolyte concentration operating capability and performance fall off was experienced. Because of this performance characteristic the product water cavity vacuum was lowered to increase the electrolyte inventory in cell No. 1. At the end of the endurance test the plaque operating electrolyte concentration had been lowered from the normal condition of 34 wgt. % KOH to 26 wgt. % KOH.

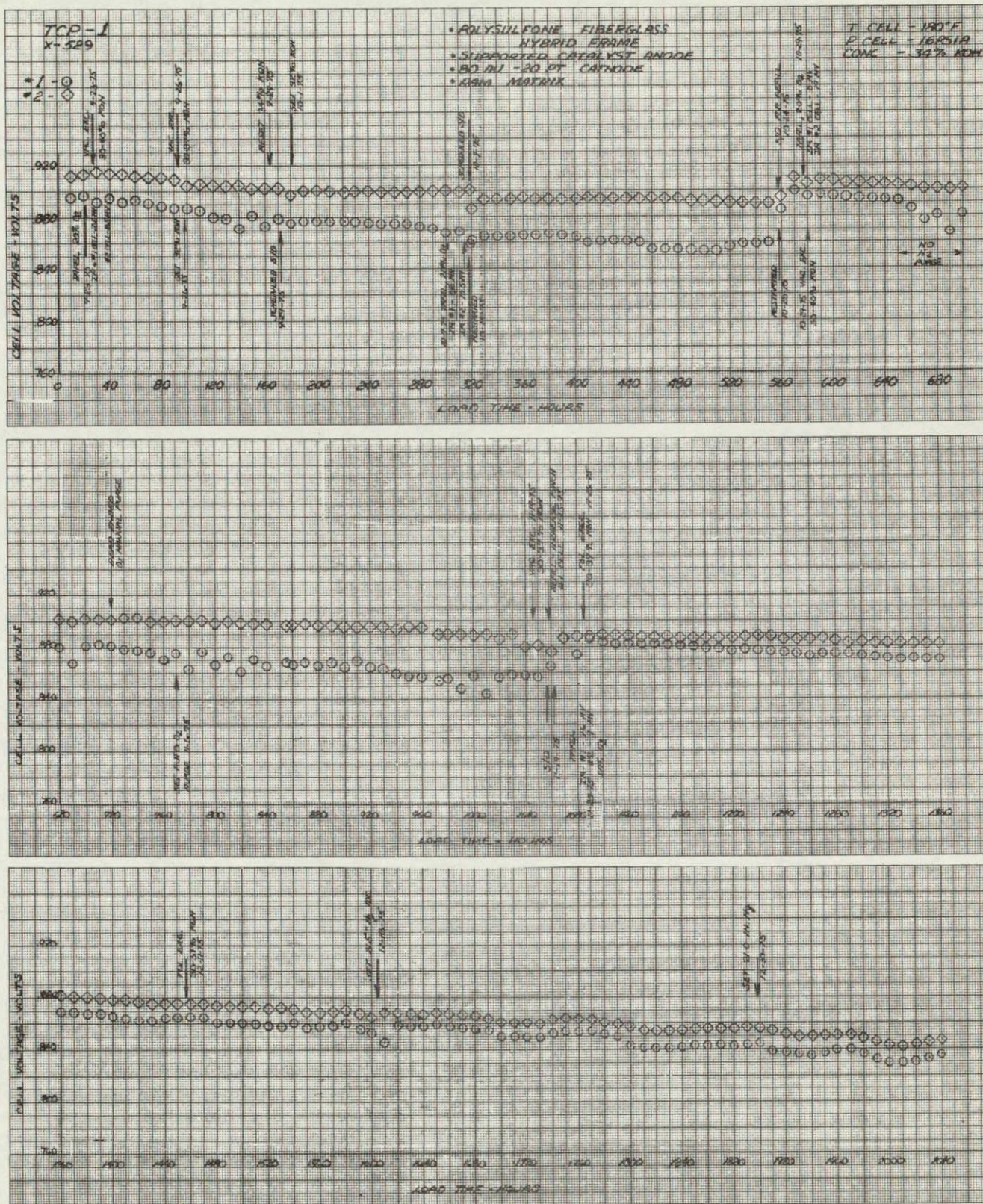


Figure 20 - Performance History, Two-Cell Plaque No. 1

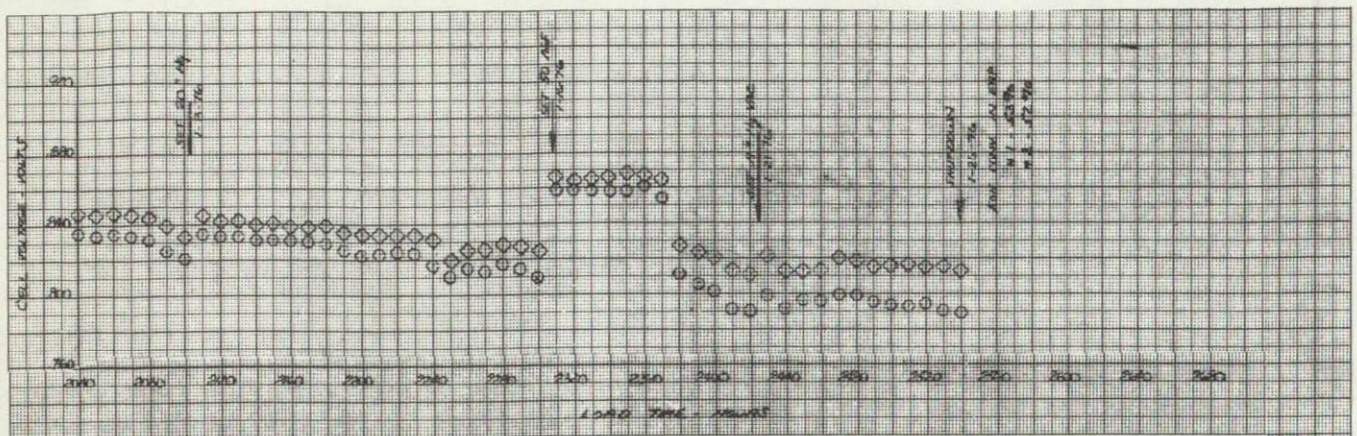


Figure 20 – Performance History, Two-Cell Plaque No. 1 (Continued)

Prior to teardown inspection the following integrity checks of TCP-1 were performed.

- | | | |
|-----------------------------|---|------------------|
| ● External reactant leakage | - | none at 10 psig |
| ● Crossover UEA | - | Both Cells |
| ● Crossover PWR | - | None at 12 psid |
| ● Reactant Flow Check | - | No port blockage |
| ● Cell to Cell leakage | - | None at 10 psid |

Figure 21 shows TCP-1 during the teardown investigation. Following removal of the oxygen side end plate small amounts of electrolyte in the bottom of the oxygen exit manifolds was observed. The following observations were made on the cell assembly.

- The ERP from Cell No. 1's UEA appeared to have gold colored plating on the anode side.
- The nickel plating on the anode side of the Cell No. 2's ERP was essentially depleted.
- The PWR unit appeared normal in all respects.
- Pinch appeared to be uniform throughout both cells.
- Both UEA ERP's appeared to be poorly plated internally.
- Cell No. 2's ERP was reasonably wettable in water; cell No. 1's ERP was not.

ORIGINAL PAGE IS
OF POOR QUALITY

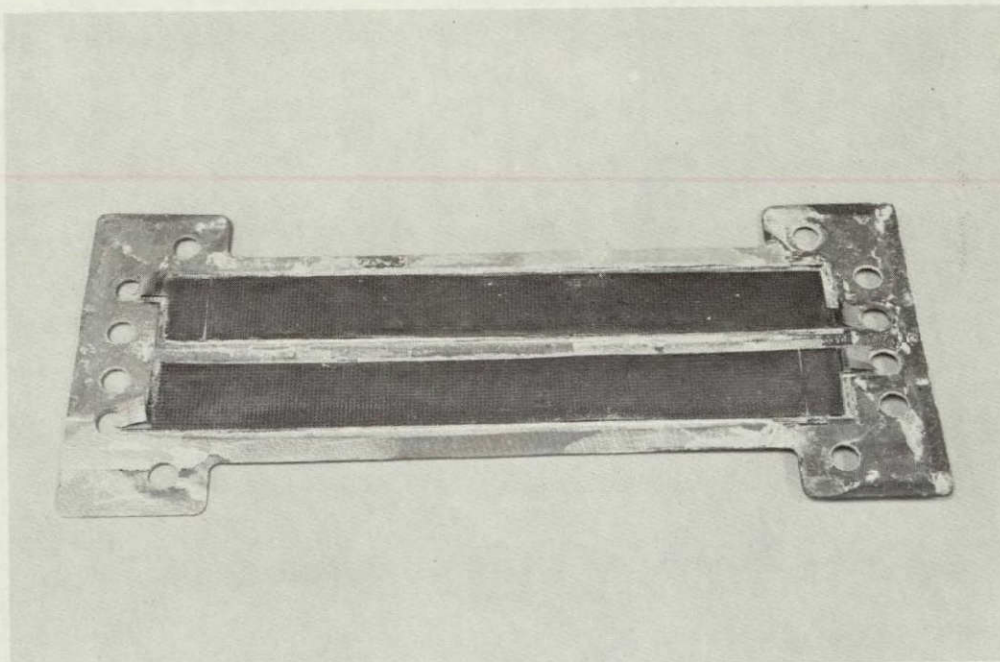


Figure 21 — Two-Cell Plaque No. 1

(WCN-4015)

Two-Cell Plaque No. 2

Two-Cell Plaque No. 2 was constructed using a hybrid frame UEA, standard PPF anodes, 90Au-10Pt cathodes, and reconstituted asbestos matrices. The plaque featured nickel Kintex flow fields in the hydrogen and oxygen cavities. The Kintex fields were selected because of their good weight and cost characteristics and low pressure drop. This plaque was fabricated and accumulated 986 hours of endurance testing during the previous contract (ref 1).

During this program an additional 1779 hours of endurance operation was acquired. A total of 2765 hours of operation at a cell temperature of 180°F (11.03 N/cm²) (82.2°C), current density of 100 ASF (107.6 ma/cm²) and a 16 psia reactant pressure. The complete performance history of TCP-2 is shown on Figure 22.

ORIGINAL PAGE IS
OF POOR QUALITY

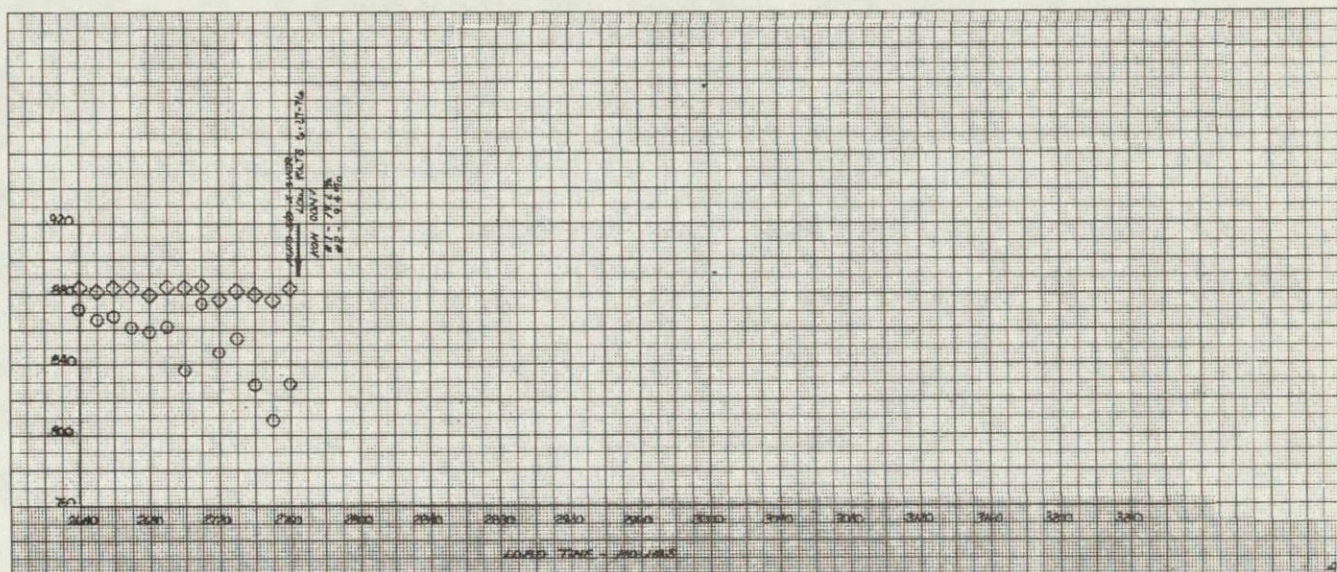
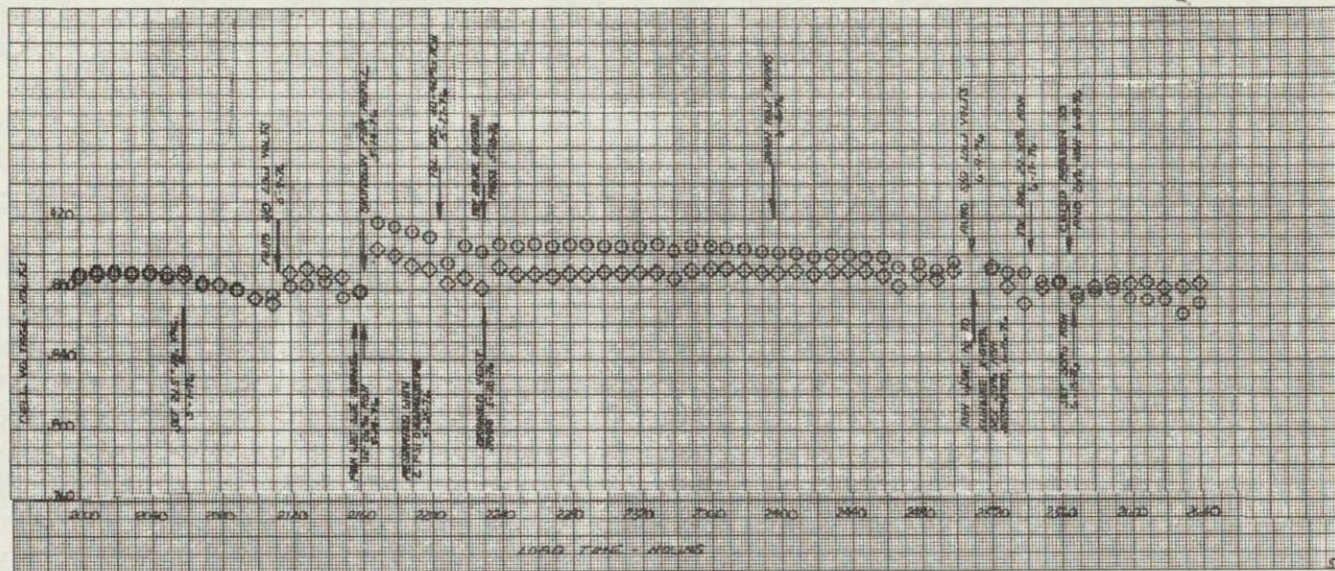


Figure 22 – Performance History, Two-Cell Plaque No. 2 (Continued)

At 986 load hours the endurance test was interrupted to install instrumentation in order to allow determination of any voltage across the polysulfane ERP of the cell. In addition, a provision was made to short the anode to the hydrogen flow field to eliminate any voltage between those components. Cell instrumentation changes, Figure 23, were made to eliminate the possibility of electrolyte being driven out of the ERP by a potential difference, electrokinetic phenomenon. Furthermore, liquid traps were installed on all exit fluid lines to recover any electrolyte exiting the cell. In order to assure proper electrolyte inventory at initiation of the endurance test, the cell was refilled with electrolyte.

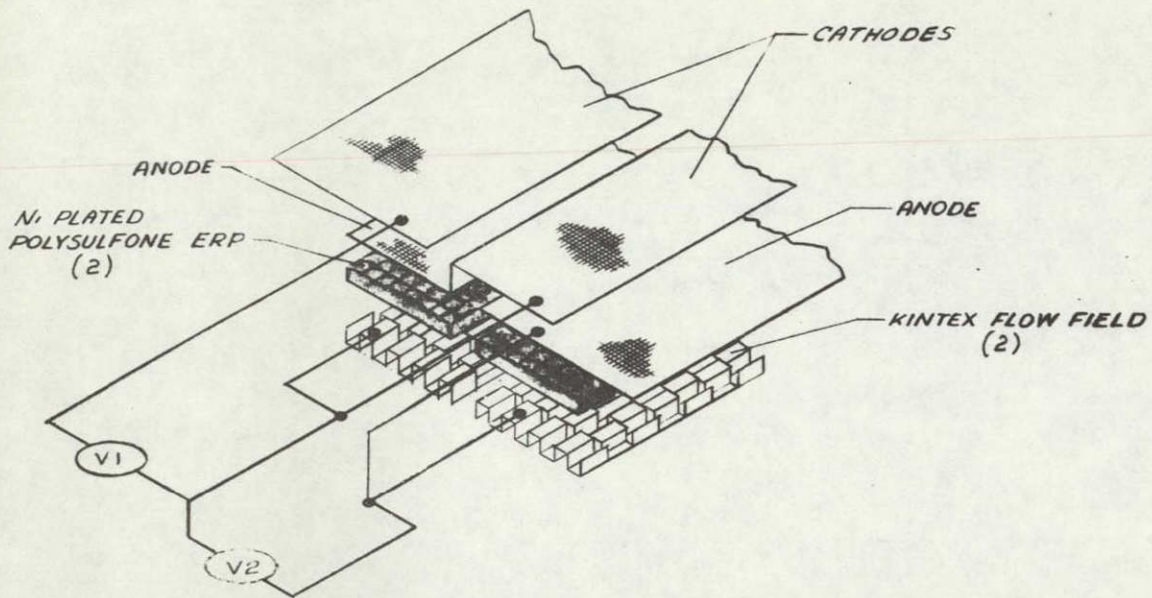


Figure 23 — Two-Cell Plaque Voltage Connections Showing Flow Field Shorted to Anodes

The endurance test was resumed with the anodes shorted to the hydrogen flow fields. The performance response to electrolyte concentration (Figures 24 and 25) was investigated shortly after setting endurance conditions. The response was normal. However, within 23 hours of the resumption of the endurance test a droop in performance upon increasing electrolyte concentration was observed. Measurement of unshorted potential across the ERP showed less than 3 mV. These test results suggest that an electrokinetic effect was not contributing the electrolyte reduction. Monitoring of the cell exit traps during operation indicated that insufficient electrolyte was lost to account for the performance droop at increased electrolyte concentrations. A summary of cell accountable performance losses is presented in Table VI.

TABLE VI
TWO CELL PLAQUE NO 2 PERFORMANCE SUMMARY

Frame Hybrid Polysulfone Epoxy Glass Fiber
 Cathode 90 Au 10 Pt
 Anode PPF
 ERP Polysulfone
 Matrix RAM
 Flow Fields Nickel Kintex

**ORIGINAL PAGE IS
OF POOR QUALITY**

Cell No	Load Time (Hrs)	PERFORMANCE			IR (mV)	Activation Loss (mV)	DIFFUSION LOSS (100 ASF)		
		10 ASF	20 ASF	100 ASF*			Total (mV)	Anode (mV)	Cathode (mV)
1	23	1 032	1 020	940	14	---	18	14	4
2	23	1 029	1 018	936	8	---	19	10	9
1	198	1 024	1 012	914	16	8	30	23	7
2	198	1 028	1 016	926	8	1	23	17	6
1	337	1 035	1 024	939	13	--	--	--	--
2	337	1 034	1 023	937	6	--	--	--	--
1	1012	1 026	1 017	935	15	6	14	7	7
2	1012	1 025	1 015	925	10	4	32	27	5
1	1231	1 028	1 017	920	22	4	--	--	--
2	1231	1.022	1 011	907	18	7	--	--	--

*Performance Corrected For Cell IR

At 1231 hours the endurance test was again interrupted for an electrolyte refill to assure proper distribution of electrolyte in UEA and PWR before continuation of testing. The plaque was remounted in the test stand with the anode side up to prevent loss of electrolyte from the ERP by gravity. The evaluation of performance response to concentration variation with load time following this refill is shown in Figure 23. As evident from Figures 26 and 27, there was an increasing performance droop with time upon changing electrolyte concentration. Analysis of reactant exit traps identified that the majority of the electrolyte was found in the oxygen trap consistent with the previous test data. At 2156 hours a special test was conducted to distinguish between a reduction in cell electrolyte inventory or lack of sufficient electrolyte movement between cell and ERP. Figure 28 presents the data from that test.

Both cells exhibited stable performance at electrolyte concentrations well below the fill concentration of 27 percent. This was an indication that electrolyte was actually lost from the UEA's, thereby creating additional volume in the ERP's which would enable the cells to operate below the fill volume without flooding. The characteristic of the cell voltage change with concentration indicated good electrolyte transfer from anode to ERP. On return to higher concentrations, the performance was normal.

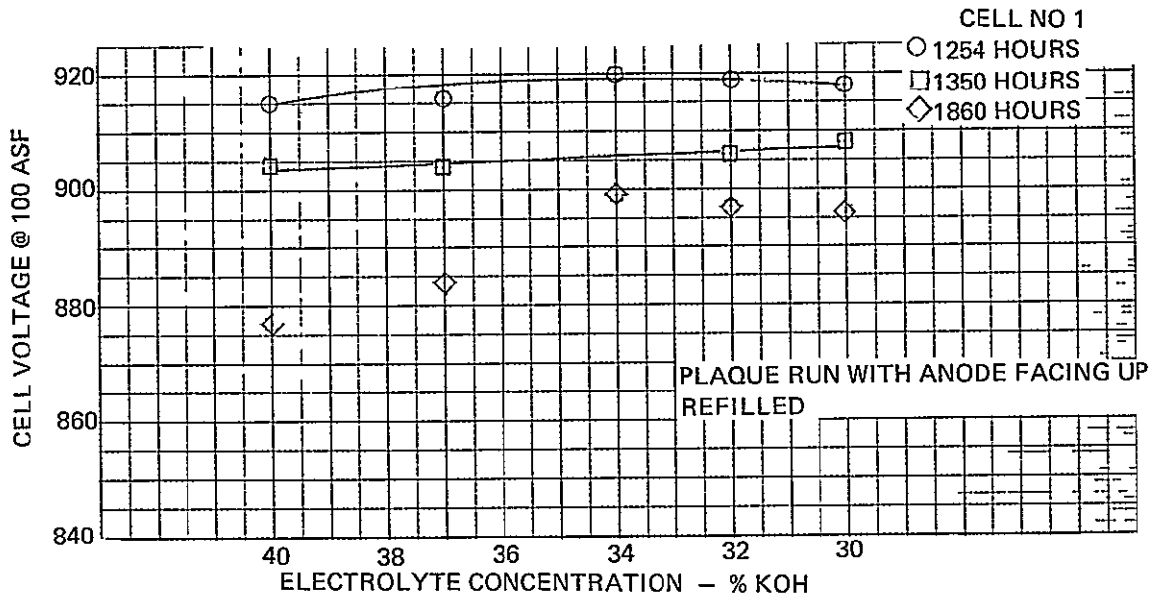


Figure 26 – Electrolyte Excursion Data, Two-Cell Plaque No 2, Cell No 1

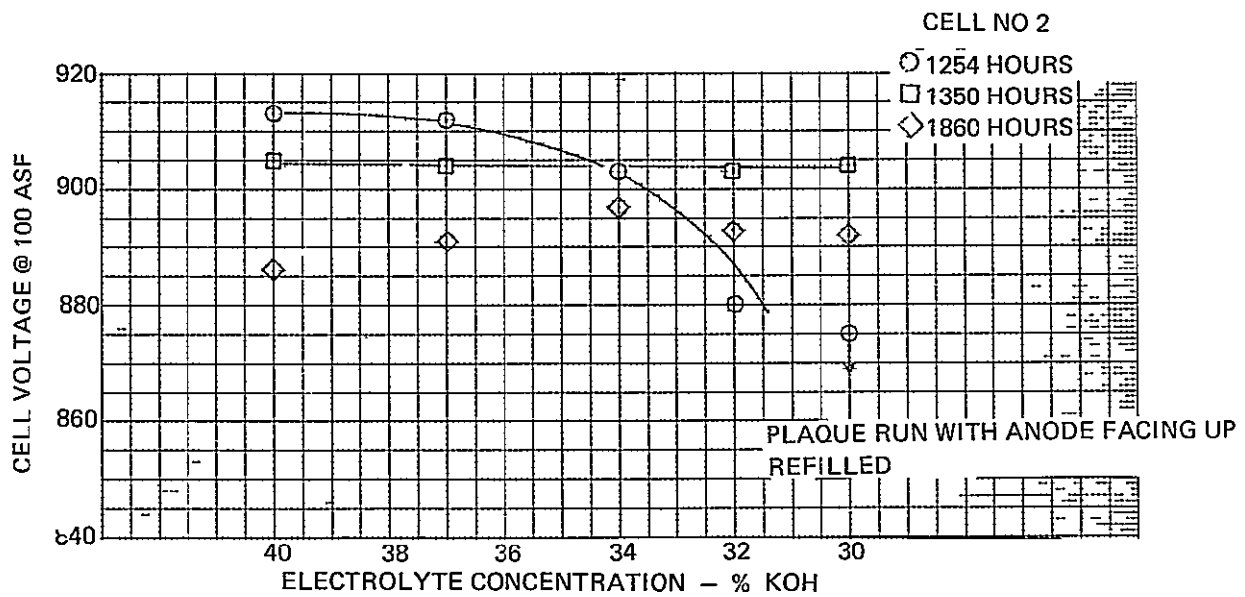


Figure 27 – Electrolyte Excursion Data, Two-Cell Plaque No 2, Cell No 2

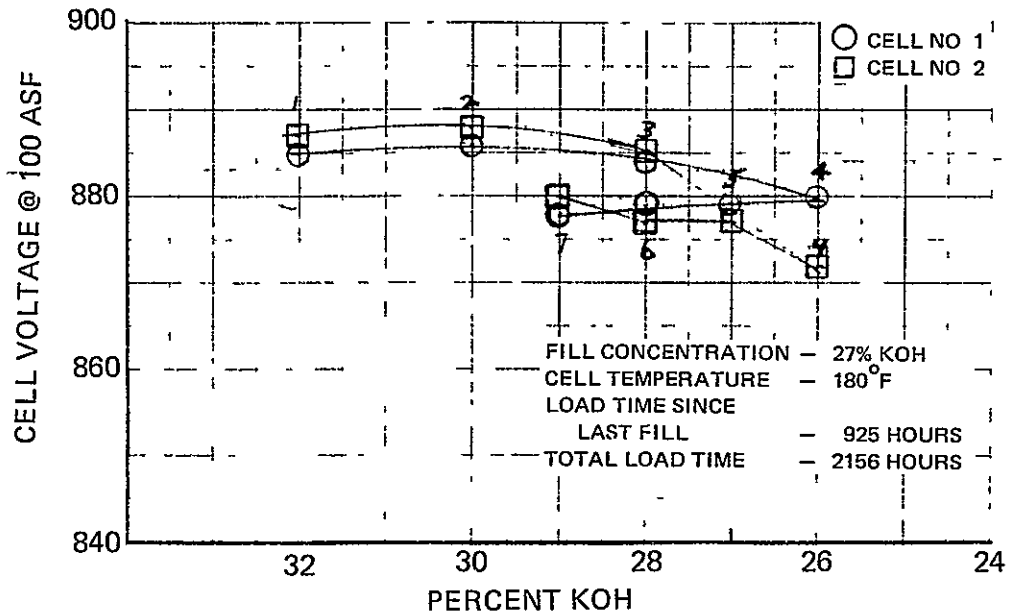


Figure 28 - Two-Cell Plaque No. 2, Wet Side Electrolyte Excursion

The endurance test was interrupted to electrolyte refill the plaque in order to establish the proper cell electrolyte inventory. Upon resumption of the endurance test a 2 psi oxygen overpressure was established to investigate if this condition would prevent electrolyte loss from the cathode. Deteriorating performance and evidence of reactant crossover necessitated that reactant pressures be equalized after only 80 additional hours of endurance operation. In an attempt to seal the crossover site the operating electrolyte concentration was reduced from 34 to 30 percent KOH thereby increasing UEA electrolyte volume. The low performance of Cell No. 1 and a possible short in Cell No. 2 forced discontinuation of the endurance test at 2765 hours.

Teardown of the plaque showed evidence of uniform pinch throughout the cells. Except for some normal darkening at the hydrogen inlet of the anode, ERP and flow field the plaque appeared to be in good condition.

Two-Cell Plaque No. 3

The construction of two cell plaque no. 3 was modified to aid in the identification of the mechanism for cell to product water removal assembly electrolyte transfer. A layout cross section of the plaque is presented in Figure 29. In place of a completely bonded assembly used in Two-Cell Plaques No's. 1 and 2, this unit was fabricated without an end cap on the oxygen side. This feature permitted the matrix compression, pinch, of the cells to be adjusted by the addition of shims to the back of the oxygen field. Silicone rubber gaskets were utilized to seal the oxygen cavity and preclude any cell to cell electrolyte transfer and external

oxygen leakage. The performance characteristics of the previous two cell plaques suggested a possibility that inadequate electrolyte wetting of polysulfone ERP's may be responsible for the electrolyte loss from the UEA. Therefore nickel ERP's which have shown consistent electrolyte wetting characteristics were utilized.

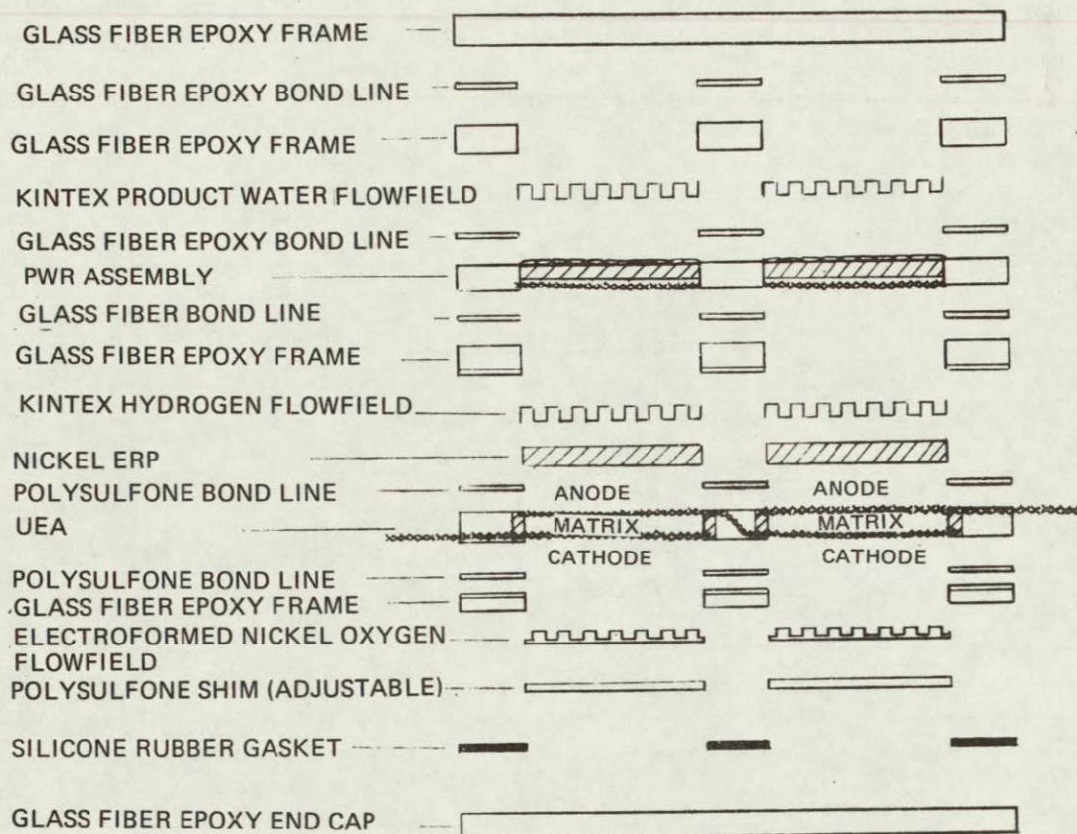


Figure 29 — Cross Section of Two-Cell Plaque No. 3 Showing Adjustable Pinch Feature

Two-Cell Plaque No. 3 was fabricated with epoxy glass fiber frames, standard PPF anodes, and 90 Au-10 Pt cathodes, and 0.010 inch (0.015 cm) thick asbestos matrices. The nickel ERP's were 0.022 inch (0.056 cm) thick and of the same design used in earlier NASA-Lewis Cells (ref 2). Other features include 0.035 inch (0.089 cm) thick nickel-Kintex hydrogen fields fabricated from 0.005 inch (0.013 cm) thick foil, electroformed-nickel oxygen fields with 0.012 inch (0.030 cm) field depth, and 0.035 inch (0.089 cm) thick Kintex water vapor transport fields.

During the contract period the plaque accumulated 2527 hours at a current density of 100 ASF (107.6 ma/cm²), 180°F (82.2°C) cell temperature and a 16 psia (11.03 N/cm²) reactant pressure. The performance history

of TCP-3 is shown in Figure 30. The performance response to concentration variation (Figure 27) at the start of the test was normal. However as the endurance test progressed there was an increasing performance droop at high electrolyte concentrations. The performance accountable losses presented on Table VII indicates that approximately half of the voltage change was in the diffusion region and the remainder due to activation loss and IR increases. The special electrolyte excursion test to distinguish between a reduction in cell electrolyte inventory or lack of sufficient electrolyte movement between cell and ERP was conducted at 605 hours and the test results are shown in Figures 31 and 32. Both cells in the plaque exhibited stable performance at electrolyte concentrations below the fill concentration which is an indication of a reduction in cell electrolyte inventory. To assure proper electrolyte inventory in the cells the endurance test was discontinued to allow an electrolyte refill of the plaque.

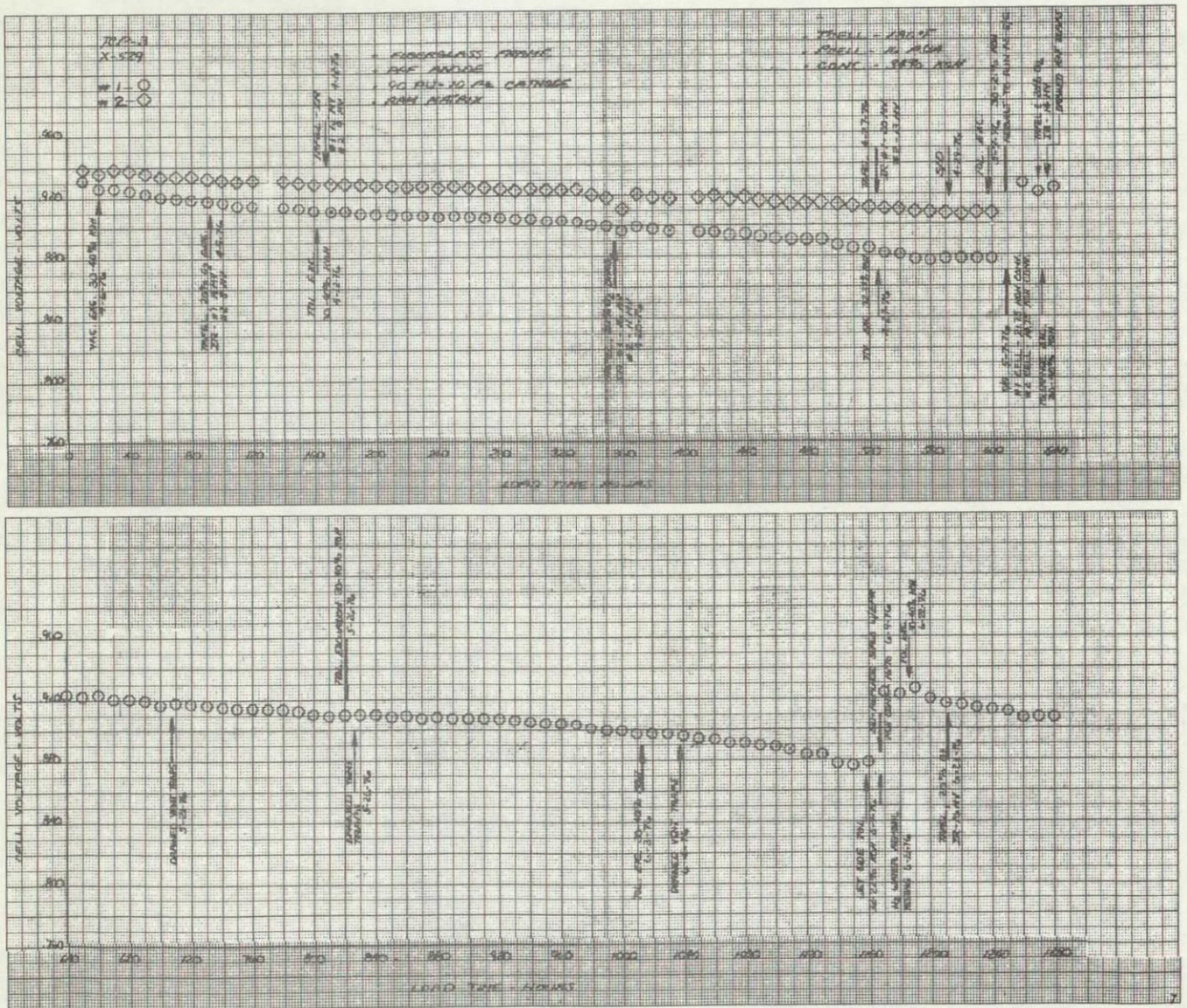


Figure 30 - Performance History, Two-Cell Plaque No. 3

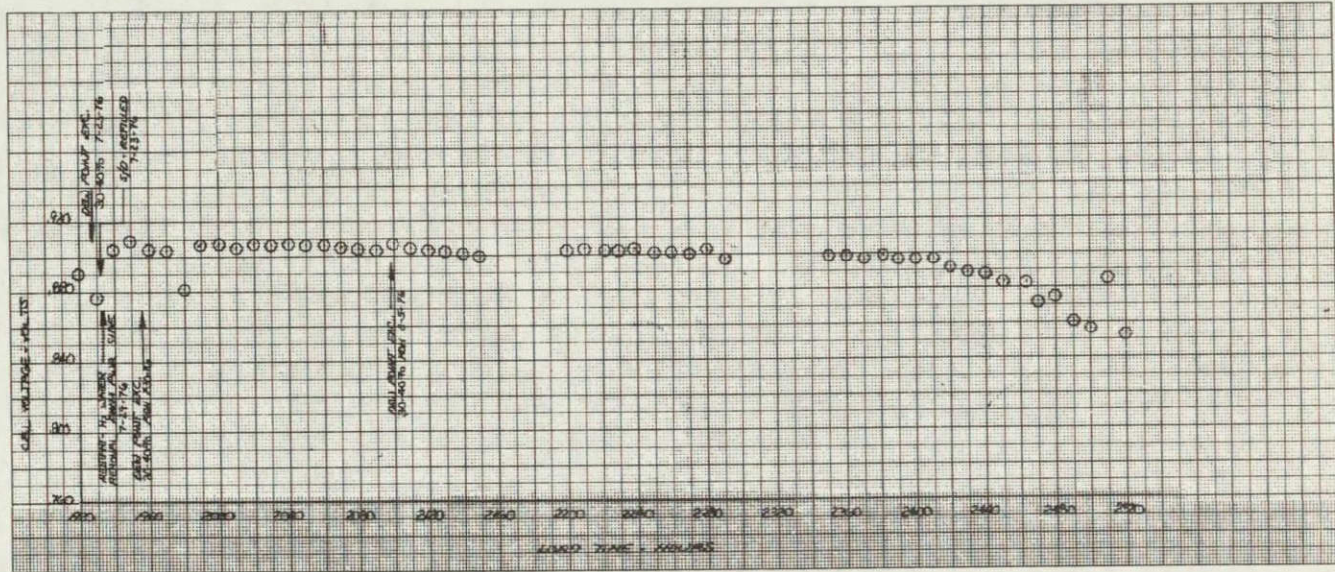
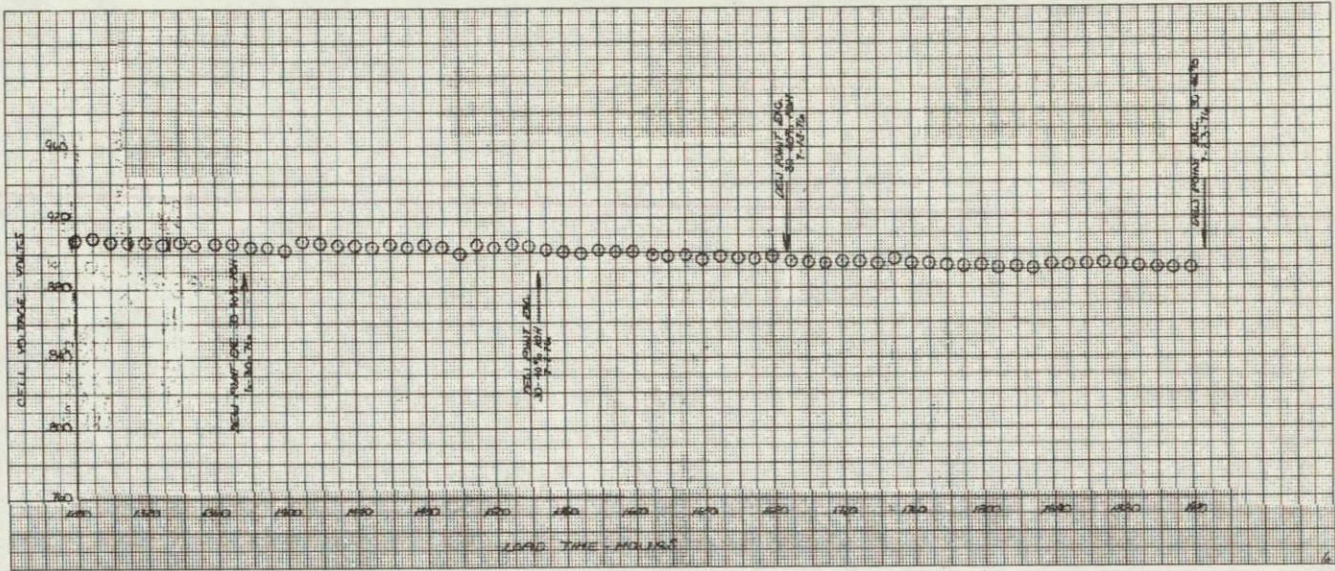


Figure 30 - Performance History, Two-Cell Plaque No. 3 (Continued)

TABLE VII
TWO-CELL PLAQUE NO. 3 PERFORMANCE SUMMARY

Frame: Epoxy-Glass Fiber
Cathode: 90 Au-10 Pt
Anode: PPF
ERP: Nickel (UEA)
Polysulfone (PWR)
Matrix: RAM

CELL NO.	LOAD TIME (HRS)	PERFORMANCE			IR (mV)	ACTIVATION LOSS (mV)	DIFFUSION LOSS (100 ASF)		
		1.0 ASF	2.0 ASF	100 ASF*			TOTAL (mV)	ANODE (mV)	CATHODE (mV)
1	92	1.034	1.022	.933	14	-	16	11	5
2	92	1.037	1.025	.941	8	-	14	8	6
1	170	1.031	1.019	.927	15	3	18		
2	170	1.035	1.024	.939	9	2	13		
1	355	1.027	1.014	.915	16	7	28	20	8
2	355	1.031	1.019	.929	11	6	24	15	9
1	523	1.025	1.014	.904	20	9	36		
2	523	1.031	1.019	.924	13	6	24		
1	630	1.035	1.024	.943	14	-	14	10	4 Refilled
1	1211	1.031	1.020	.934	16	-	20	16	4 Refilled

*Performance Corrected For Cell IR

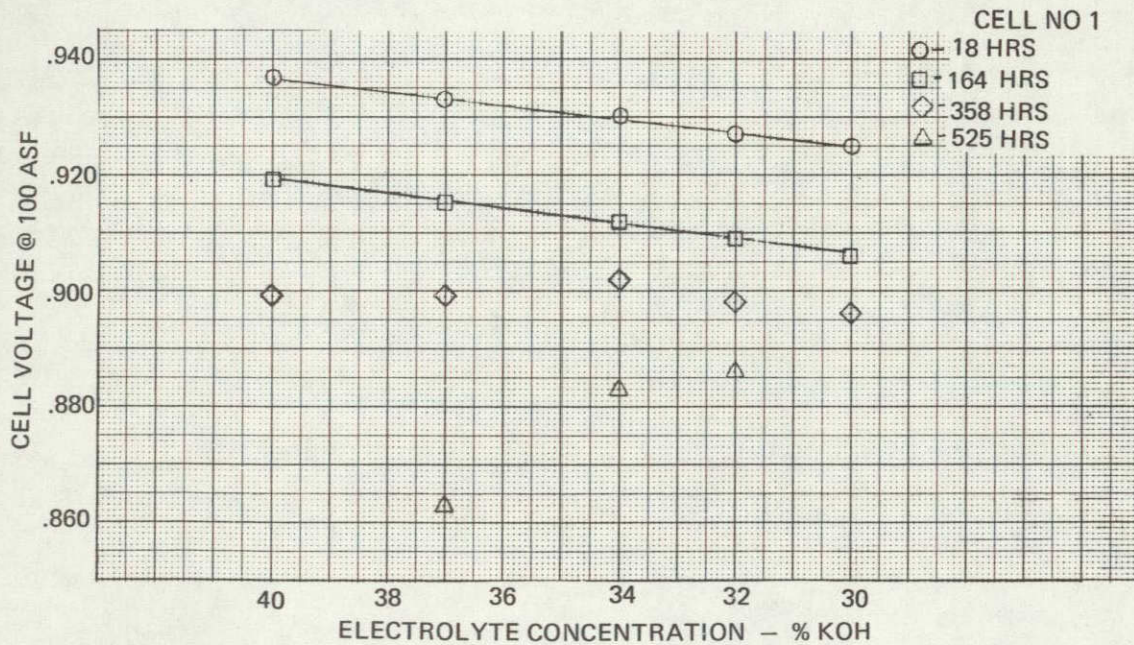


Figure 31 - Electrolyte Excursion Data Two-Cell Plaque No. 3, Cell No. 1

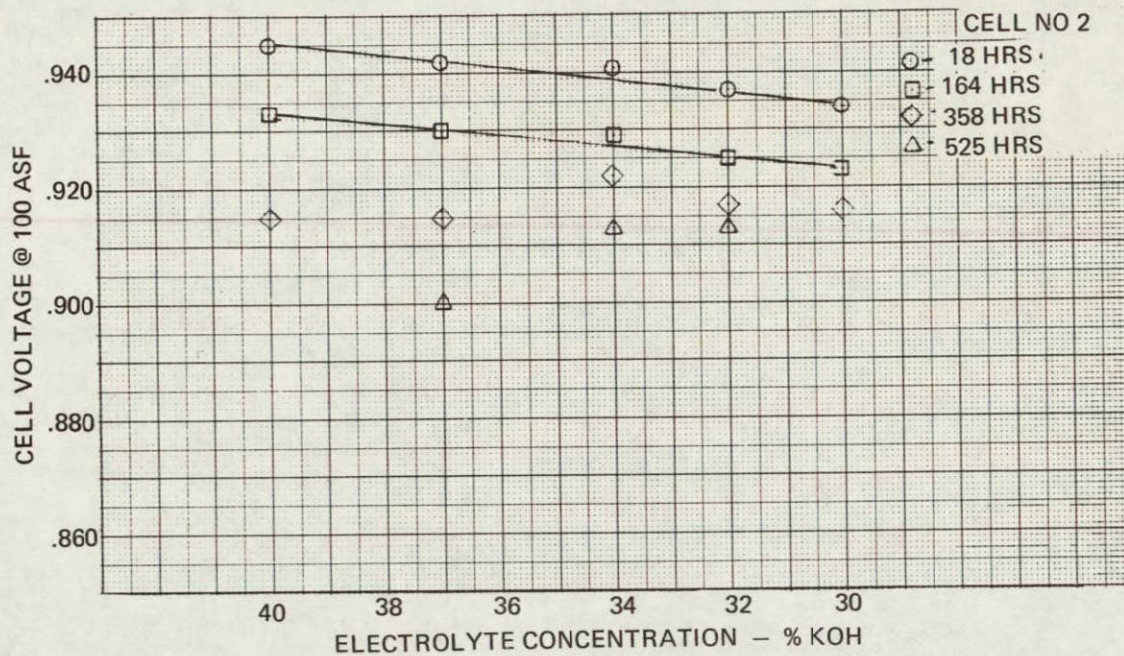


Figure 32 – Electrolyte Excursion Data, Two-Cell Plaque No. 3, Cell No. 2

During the shutdown the plaque as modified to allow operation of cell No. 1 as a single cell. The purpose of this test configuration was to determine if the increasing performance droop during the electrolyte excursion testing was related to the higher voltage of cell during plaque operation or a unknown characteristic of the two-cell plaque design. The performance characteristics and test data from electrolyte concentration excursion testing were similar to those observed during early endurance operation. The similarity of the performance characteristics between single cell operation and two-cell plaque operation indicated that voltage was not a factor in the reduction of cell electrolyte inventory. Figure 33 shows the performance history of cell No. 1 superimposed on the cells performance during two-cell plaque operation. The results of electrolyte concentration testing is shown in Figure 34.

At 1167 hours the endurance test was interrupted to conduct an electrolyte refill to assure proper distribution of electrolyte between the cell and PWR unit. Upon resumption of the endurance test the PWR unit was isolated from the cell to determine if improper PWR operation caused by laminating cycles could be contributing to reduction in cell electrolyte inventory with time. This was done by dead-ending the water-vapor field and removing the water by flowing hydrogen through the hydrogen gas cavity. A saturator was added to the hydrogen system to maintain the proper inlet dew point. The water vapor cavity now operated at ambient pressure. A more stable performance characteristics was experienced as shown on Figure 35.

ORIGINAL PAGE
OF POOR QUALITY

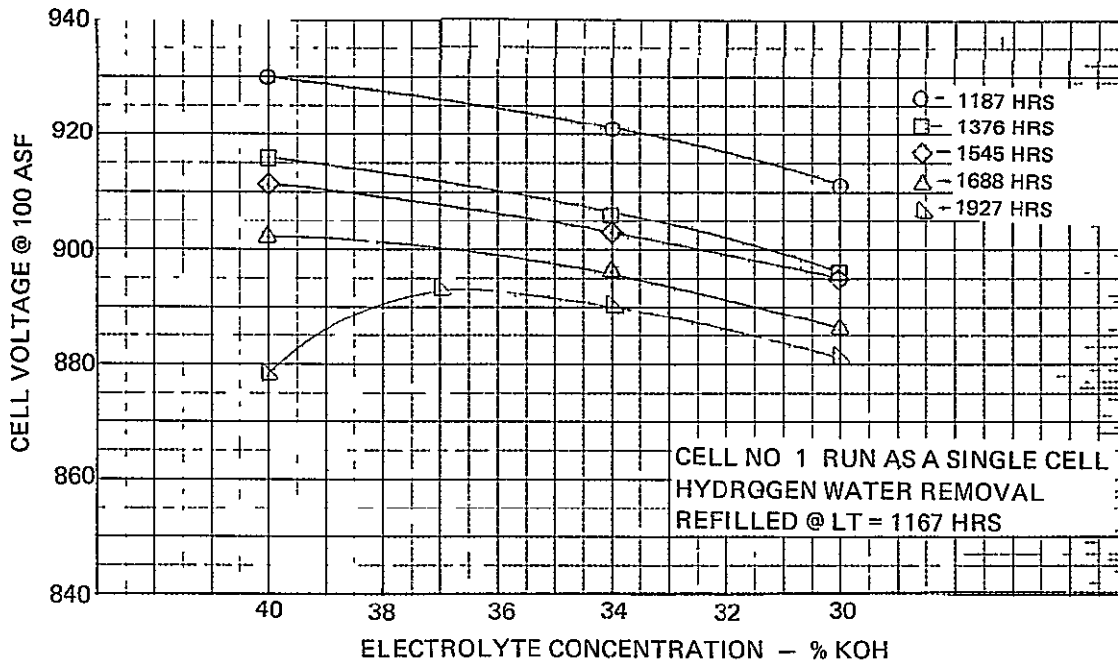


Figure 34 - Electrolyte Excursion Data, Two-Cell Plaque No 3, Cell No 1

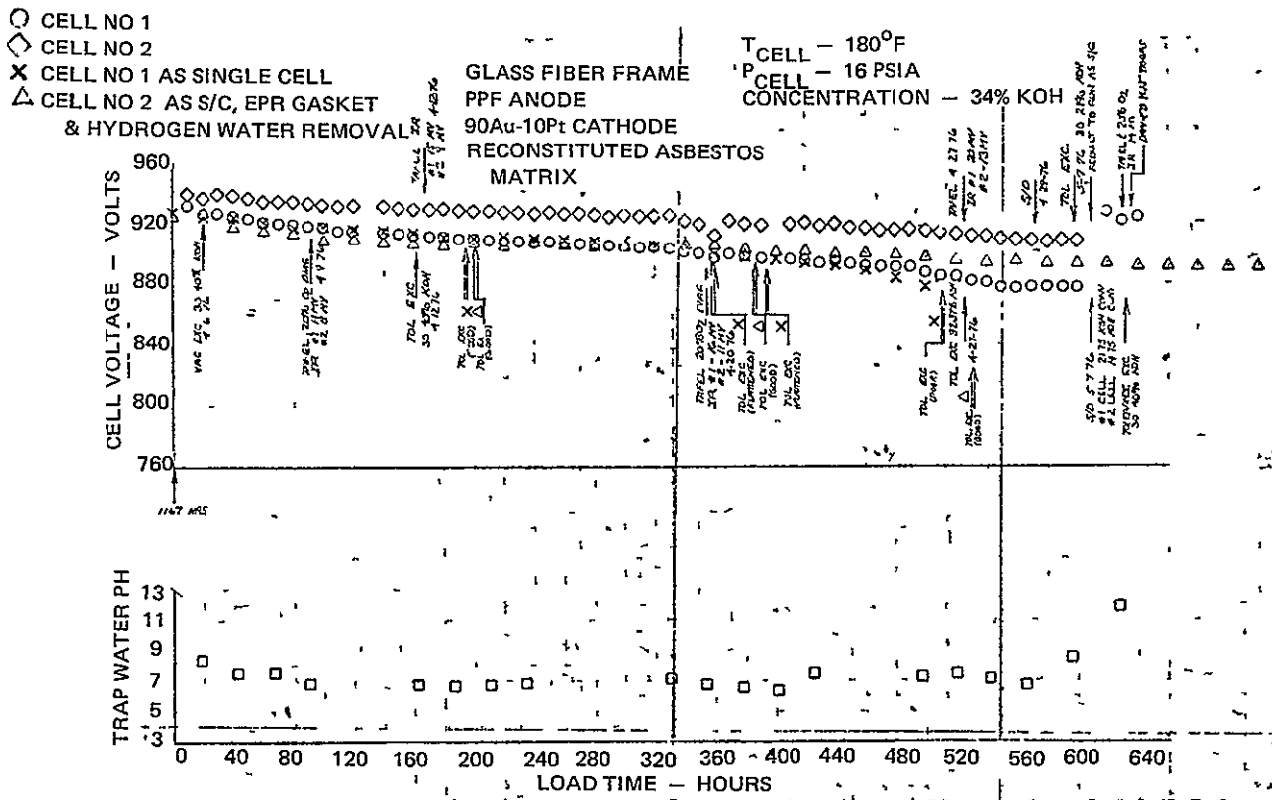


Figure 35 - Performance History, Two-Cell Plaque No 3

Test data from electrolyte excursion tests is presented in Figure 36. As shown over 500 hours elapsed before the performance droop with increasing electrolyte concentration was experienced. In previous electrolyte excursion tests with a functioning PWR unit, the cell normally exhibited a performance droop in 350 load hours following an electrolyte refill. This information suggests that the PWR unit was a component of the cell electrolyte inventory reduction process. Endurance operation was interrupted at 1932 hours electrolyte refill the cell to obtain the correct cell electrolyte inventory.

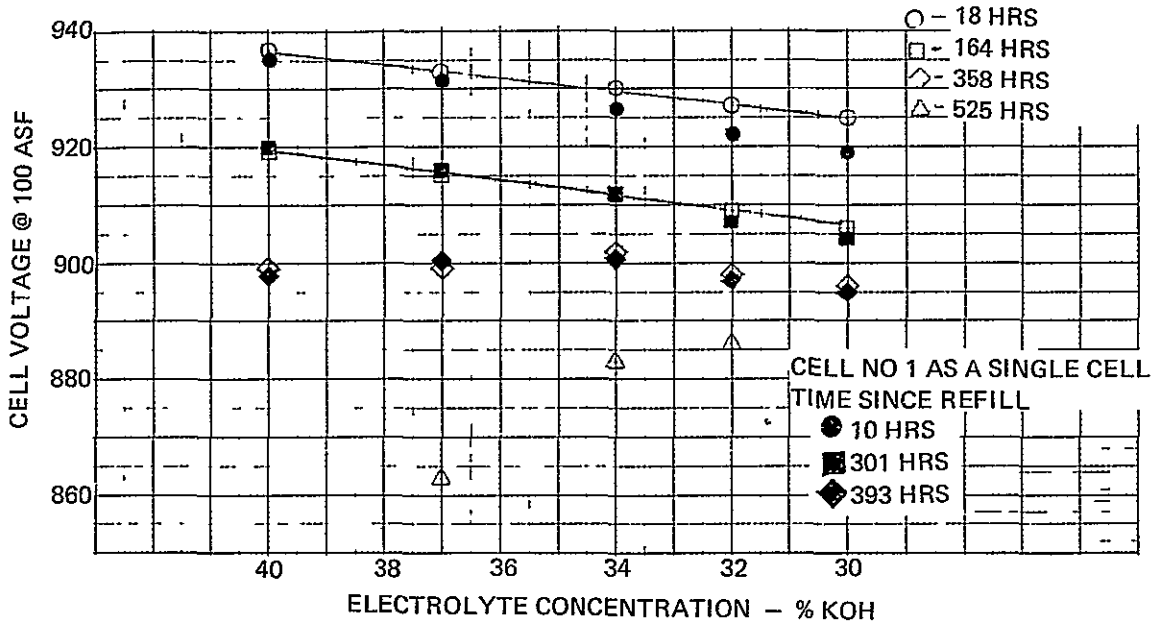


Figure 36 — Electrolyte Excursion Data, Two-Cell Plaque No 3

The test stand was modified to permit product water removal by flowing hydrogen through the PWR water cavity. This method of product water removal simulates actual operation of the PWR unit without the large pressure differential of normal operation. This eliminates the pressure differential (Appendix B) as a mechanism of driving electrolyte from the UEA and PWR thereby reducing cell electrolyte inventory. An improvement in the performance history was noted upon resumption of the endurance test. The results of electrolyte excursion tests are shown in Figure 37. As shown there was a performance droop with increasing electrolyte concentration at 482 hours. This data suggests that electrolyte transfer had occurred, however, there was an incident where the cell was flooded from an over flow of the hydrogen inlet water trap at 2270 hours of total endurance operation. This incident could have washed electrolyte out of the cell resulting in a reduction of cell electrolyte inventory.

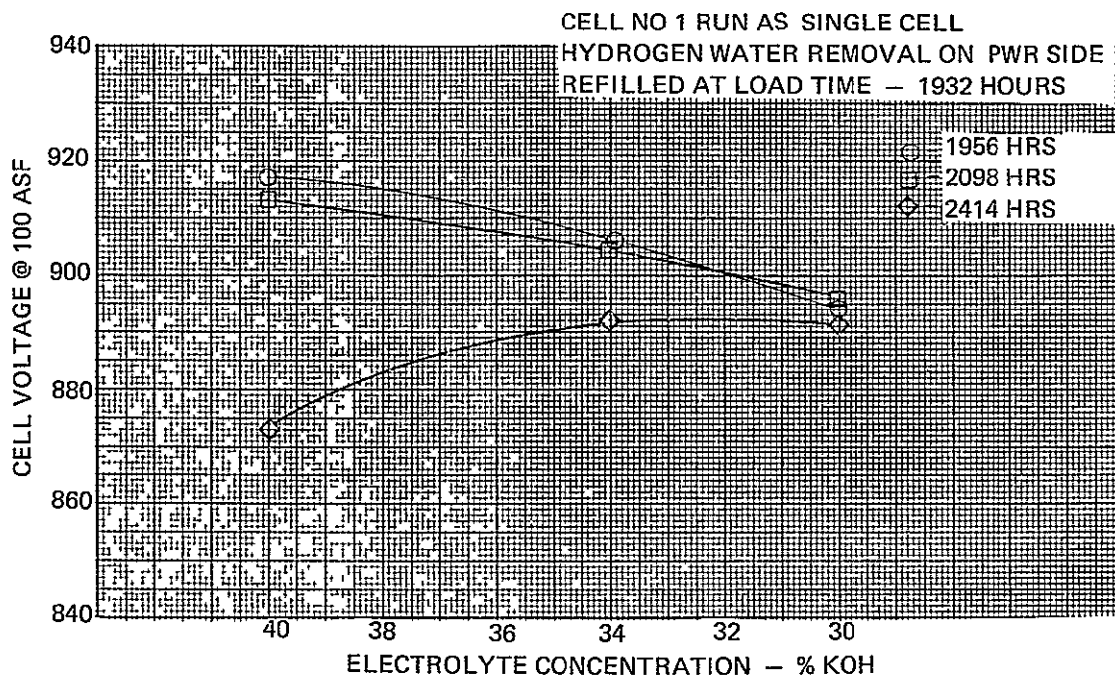


Figure 37 - Electrolyte Excursion Data, Two-Cell Plaque No 3

The onset of reactant crossover at 2527 hours of endurance operation forced termination of further testing.

Disassembly of the cell showed some electrolyte entrained behind the electroformed-nickel oxygen field. Analysis showed however that the amount was only 10 percent of that required to cause electrolyte transfer symptoms, therefore this was ruled out as a possible contribution to the transfer problem. A hydrogen overpressure is suspected to be the most probable cause of the electrolyte entrainments

19

APPENDIX A
BASE CELL ELECTROLYTE LOSS

A-1

APPENDIX A

BASE CELL ELECTROLYTE LOSS

INTRODUCTION AND SUMMARY

Recent base cell tests indicate an apparent loss of electrolyte. This study was begun to determine possible mechanisms to explain this loss. In one of these mechanisms, the pressure difference across the passive water removal assembly forces electrolyte from the anode ERP to leak out across films of electrolyte covering the hydrogen flow field separator. The calculated rate of electrolyte loss to be expected from this mechanism is of the order of the rate observed experimentally. As a result of these calculations, it is recommended that only non wetting materials be used for hydrogen flow field separators.

MECHANISM OF ELECTROLYTE LOSS ALONG FILMS

Originally, all of the porous solids in the cell are filled with 27 percent KOH. Water is evaporated from this solution until the concentration is 34 percent in all parts of the cell. The volume after evaporation is calculated from the ratio of the concentrations times the densities. Because of their small size, the pores in the matrices and electrodes are not emptied by evaporation. Practically all of the volume change occurs in the ERPs reducing their filled volume from 4 cm³ to 2.5 cm³, and therefore reducing their saturation from one to 0.63. The displacement pressure difference corresponding to this saturation is found from the displacement curve to be 2.5 psi. Since the surface tension of 34 percent KOH at 180°F is nearly the same as the surface tension of water at room temperature, the displacement and imbibition curves for water in the ERPs were used without modification. The pressure in the electrolyte in the ERP will be 2.5 psi less than the 16 psi in the hydrogen flow field, or 13.5 psia.

The pressure in the liquid in the matrix will also be 13.5 psia. If the displacement curve for the matrix were known, the saturation of the matrix would be the value corresponding to a pressure difference of 2.5 psi. This value is assumed to be close to one, and is denoted by $1-\sigma$.

Due to the fill procedure, a thick film of electrolyte will cover the surface of the Kintex or other wettable hydrogen flow field separator. The pressure in the film will be 16 psia, but the pressure in the adjoining porous solids is only 13.5 psia. Liquid will drain first from the region touching the porous solids and later from the entire thick film until liquid remains only in irregularities and microgrooves with radii

$$r \cong \frac{\sigma}{\Delta P} 4.10^{-4} \text{ cm.}$$

Microgrooves at least as large as $0.5 \cdot 10^{-4}$ cm, or 0.5 microns, must exist because the Kintex is not shiny and because a piece of metal will appear shiny if, and only if, the dimensions of the surface roughness are less than

the wavelength of light, which is about 0.5 microns. These saturations and pressures are summarized in Figure A-1 for the case where the pressure is 16 psi in both the hydrogen flow field and the product water cavity.

The effect of reducing the partial pressure in the product water cavity to 4 psia is shown in Figure A-2. This pressure drop across the matrix is much less than is required to cause breakthrough. Since the 12 psi pressure difference is much greater than the original 2.5 psi pressure difference, a small amount of electrolyte will leak out into the PWR ERP. The saturation of the matrix will still be close to one and is denoted by $1-\epsilon$. The meniscus at the interface between the matrix and the ERP will be flat and the pressure in the liquid will be equal to the pressure in the gas in the ERP. Gas is present in the ERP because the ERP is in the breakthrough condition. The entire 12 psi pressure drop occurs across the meniscus facing the hydrogen flow field.

The pressure in the liquid drops linearly across the Kintex. The gas-liquid pressure difference remains 2.5 psi on the UEA side of the Kintex, but increases to 12 psi on the PWR side. Only surface roughness having a radius less than 0.9 microns is occupied by liquid near the PWR side. A groove on the PWR side having a circular cross-section of 0.5 micron will have a meniscus of radius 0.9 micron and therefore will be 74 percent full on that side.

The saturation of the PWR ERP is nearly at its starting value, 0.63. Therefore, the gas-liquid pressure difference is 2.5 psi and the liquid pressure is 1.5 psia. Since this pressure is below the vapor pressure of the solution, vaporization will redistribute the liquid so that it will be in cavities bounded by surfaces of no net curvature. The formation of these surfaces will raise the liquid pressure to 4 psia as is shown in Figure A-3.

Liquid will flow from the UEA-ERP through the surface irregularities on the nickel Kintex, driven by the pressure difference across the two ends of the film. After 200 hours, it is observed that about 0.8 cm^3 is lost from the UEA ERP. This transfer results in the condition shown in Figure A-4. The PWR ERP acts as a sponge to take up liquid, and its saturation increases to 0.83 with no change in pressure. The saturation of the UEA ERP decreases by the same amount to 0.43 and the gas-liquid pressure difference increases to 3 psi, making the liquid pressure 13 psia.

Allowing the flow to continue would lead to the equilibrium condition shown in Figure A-5. The PWR ERP would be filled and a small amount of electrolyte would enter the Teflon membrane. The pressure in the liquid would be greater than the pressure of the gas in the Teflon membrane because it is non-wetting. The saturation of the UEA ERP would decrease to 0.26 and the pressure in the liquid would decrease to 11.6 psia, as determined from the ERP displacement curve. The liquid pressure would be the same in all parts of the cell and no more flow will occur.

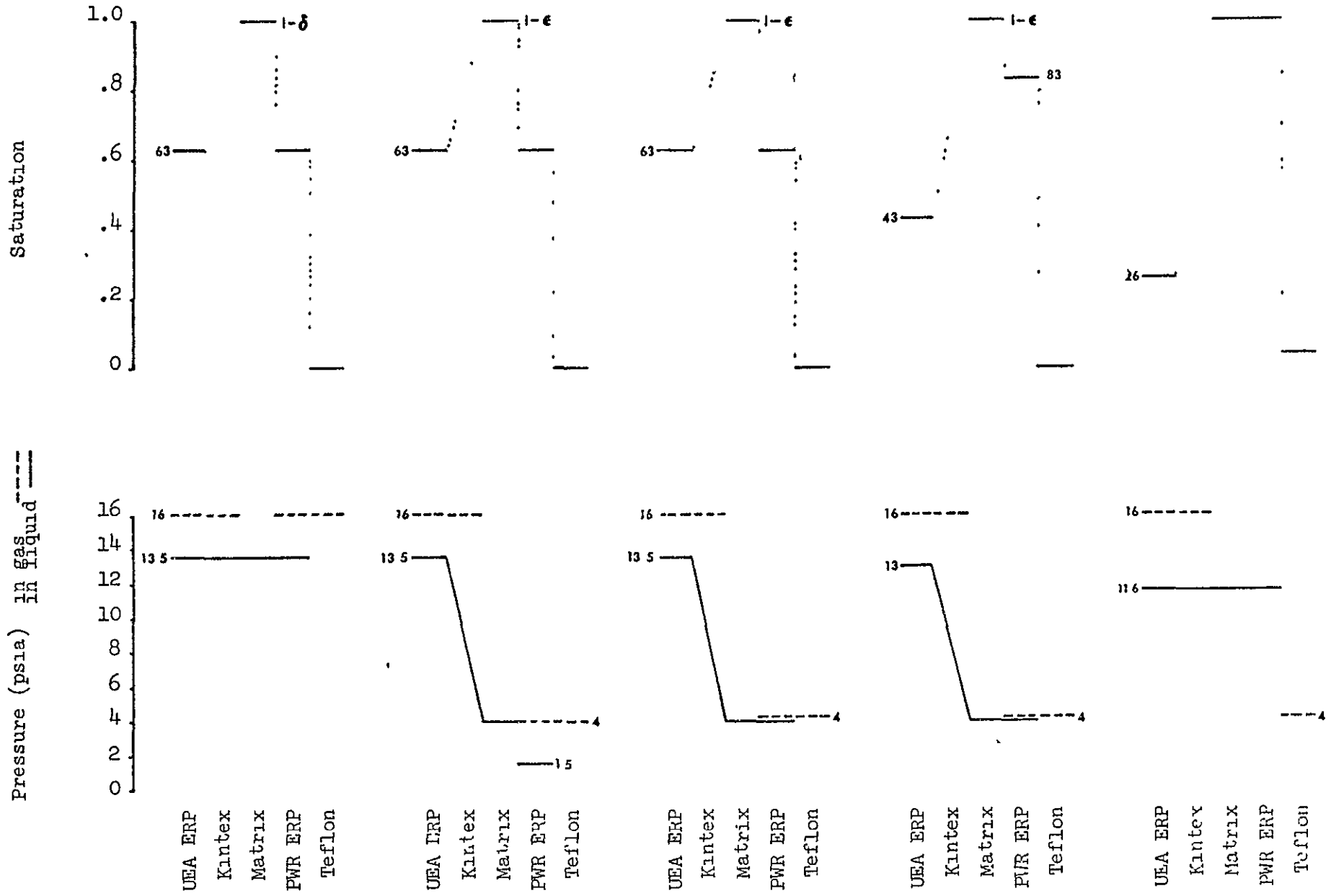
Both sides at 16 psia total pressure

Pressure reduced to 4 psia in water field

Shortly after Fig. A-2

After transfer of .8 cm³ of electrolyte

At equilibrium



Pressure/Saturation Summary

Fig A-1

Fig A-2

Fig A-3

Fig A-4

Fig A-5

COMPARISON OF EXPERIMENTAL AND THEORETICAL LOSS RATES

The rate of electrolyte loss can be estimated from experimental data in the following way. The maximum in the tolerance curve of TCP-3 at 358 hours is at 34 percent KOH. If it is assumed that the maximum at 164 hours occurs at 40 percent KOH and that the volume of the solution lost is the difference in volume between these two solutions, then the rate of drainage is 0.8 cm^3 in 194 hours or $10^{-6} \text{ cm}^3/\text{sec}$.

In the mechanism described above, electrolyte flows in surface irregularities with a depth of about 0.5 micron. A calculation of the rate of viscous flow for a uniform flat film should overestimate this flow. The quantity, Q , of electrolyte with viscosity, $\mu = 0.01$ poise, flowing through a uniform flat film of width, $w = 10 \text{ cm}$, and depth, $d = 0.5$ micron, under a pressure gradient, dP/dx of 9.5 psia per 39 mils is

$$Q = \frac{wd^3}{3\mu} \frac{dP}{dx} = 10^{-4} \text{ cm}^3/\text{sec}.$$

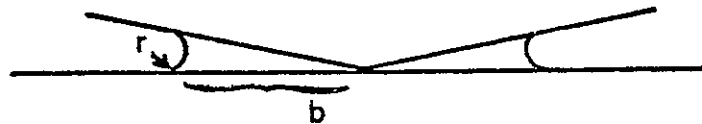
This is one hundred times greater than the rate required to match the experimental flow of $10^{-6} \text{ cm}^3/\text{sec}$. When allowance is made for the roughness of the surface, the calculated flow could easily account for the observed loss of electrolyte. In any case, substantial amounts of electrolyte will be lost when wettable separators are used.

RECOMMENDATION

On the basis of these calculations, it is recommended that non wetting separators be used in the hydrogen flow field.

ELECTROLYTE HELD IN OXYGEN FLOW FIELD

The sharp-angled juncture around the welds on the electroformed nickel oxygen flow field could take up electrolyte from the electrodes if it were not filled during the original electrolyte loading process:



The mean radius is ρ is related to the radius r by

$$\frac{2}{\rho} \sim \frac{1}{r}$$

The mean radius is obtained from the pressure differential ΔP

$$\rho = \frac{\sigma}{\Delta P}$$

where σ is the surface tension 71 dynes/cm and $\Delta P = 2.5$ psi.

Therefore, the radius is given by

$$r = \frac{\sigma}{2\Delta P} = \frac{71}{2(2.5) 68947} = 2.1 \cdot 10^{-4} \text{ cm}$$

The volume of this region is approximately (for $b = 2$ cm)

$$V \sim \frac{2}{3} \pi r b^2 = 3.4 \cdot 10^{-3} \text{ cm}^3$$

The number of welds required to give the observed 0.8 cm^3 loss in KOH is

$$n = \frac{0.8}{3.4 \cdot 10^{-3}} \sim 300,$$

which is many times larger than are used in a cell. Retention of electrolyte in the backing of the electroformed nickel does not account for the observed electrolyte loss in these cells.

APPENDIX B
ELECTROLYTE RESERVOIR PLATE
IMPROVEMENT PROGRAM

APPENDIX B ELECTROLYTE RESERVOIR PLATE IMPROVEMENT PROGRAM

INTRODUCTION

As a result of the poor wettability of the Electrolyte Reservoir Plater (ERP) in the first two-cell plaque, a program was initiated to improve the quality of the nickel plating on the polysulfone ERP's. This plating which is necessary to provide wettability is applied by a four-part electroless plating process. The process involves the following steps:

- Cleaning
- Sensitization
- Activator Cycle
- Nickel Plating

In this program the concentration and amounts of the various solutions were selectively varied to determine where improvements might be achieved. The ERP's would be subjected to several inspection methods such as visual inspection, weight pick up, electrical resistance, water take up, and electrolyte take up. The objectives of the program were:

- Improve Electrolyte Retention
- Increase ERP Uniformity

BACKGROUND

Evaluation of endurance test data and post-test analysis indicate that the most probable cause of the dry-side tolerance difficulty during Two-Cell Plaque No. 1 endurance test was poor nickel plating of the polysulfone ERPs. This could not only result in an incomplete electrolyte fill, but may have contributed to a loss of KOH during the test. Reduction of the electrolyte inventory in the ERP may have been an irreversible process. The electrolyte might not re-enter the non-wettable portions of the ERP and would be forced to the ERP surface where it would remain or be forced out the reactant exit ports or drip onto the PWR unit. The over-all result would be a loss of electrolyte experienced by a loss in dry-side electrolyte concentration operating capability.

The appearance of the ERP of Cell No. 1 in Two-Cell Plaque No. 1 differed considerably from that of Cell No. 2 and neither appears to be normal compared to a new surface (visible only under magnification). The ERP from Cell No. 1 was very dark in color, particularly on the field side, with very visible deposits of a yellow-colored material. It was also apparent that the part was very poorly plated in its interior. The ERP from Cell No. 2 had very little nickel plate on the field side and the opposite side appeared more nearly normal, albeit somewhat dark and with greater amounts of yellow-colored material. The interior of this piece contained a considerable amount of nickel

Samples of the ERP's were first tested with dilute nitric acid to determine if yellow-colored material was soluble. The nickel plate was completely removed from a new ERP in about 20 seconds, leaving white polysulfone base material. The plate was removed from the ERP from Cell No. 2 in about 30 seconds leaving a very light tan appearance. The sample from Cell No. 1 remained in the acid for 5 minutes and the field side still contained a layer of black material. In all cases the yellow-colored material was dissolved completely, although at a lower rate than the gray nickel deposit. On ERP No. 1 there was a rapid initial reaction that nearly ceased after 30 to 60 seconds; the remaining material being black in color and apparently quite compact. The black material is quickly soluble in dilute aqua regia.

A sample of ERP No. 1 was sent to United Technologies Research Center (URTC) for qualitative electron microprobe analysis to determine the elements present in the yellow material. The results showed that the major components were nickel and phosphorous, with a number of minor tract materials. Thus it appears that both the yellow material and the black material which was insoluble in HNO_3 , are phosphides of nickel resulting from improper application of the nickel plate.

A test was run to determine if electrolyte could be forced from the polysulfone ERP by voltage impressed across the ERP such as might be encountered in the two cell plaque. A plug section was removed from Cell No. 1 containing the cathode, matrix, anode, and ERP. This section was filled with the appropriate amount of 34 percent KOH and held between a metal plate on the cathode side and a screen on the ERP side (held together by a C-clamp with a plexiglass sheet above the screen so that the surface of the ERP could be seen). Gold current and voltage tabs were inserted on each side of the ERP. Current was impressed on the sample so that a voltage could be applied across the ERP. Voltages as large as 100 mV were measured across the ERP and were maintained for about 2 hours. No evidence of any electrolyte movement out the back of the ERP was visible. This was repeated with the filled ERP alone with the same results. This test appears to indicate that an electrokinetic mechanism is not responsible for the loss of electrolyte observed in TCP No. 1.

Electrolyte take-up measurements (ETU) were made on pieces of the ERP's from Cell's No. 1 and 2 and a new well plated ERP which had the appearance of a good nickel plating operation. The theoretical electrolyte volume of the ERP is $0.038 \text{ cm}^3/\text{cm}^2$. The ETU was reassured in three ways. 1) floating on 35 percent KOH, 2) evacuated under 35 percent KOH and 3) soaked under 35 percent KOH and drained which approximates the cell fill procedure (all at room temperature). The measured ETU is shown in Table B-1.

TABLE B-1

MEASURED ETU

		ERP Cell No 1	ERP Cell No 2	New ERP
Float	$(\text{cm}^3/\text{cm}^2)$	0 0125	0 0278	0 0243
Evacuate	$(\text{cm}^3/\text{cm}^2)$	0 0355	0 0328	0 0330
Drain, soak	$(\text{cm}^3/\text{cm}^2)$	0 0132	0 0243	0 0330

Cell No. 1 ERP clearly has a lower ETU than either of the other two samples. If the ERP's were filled with 27 percent KOH and dried to 34 percent KOH the volume remaining in the ERP would correspond to a fill of 10, 46, and 38 percent respectively. It was also observed qualitatively that when the samples were floated on KOH, the back of the sample became wet almost immediately in the case of ERP No. 2 and the new sample, but no electrolyte was observed on the back of Sample No. 1 except for a little on the edge where the sample had been cut. Apparently the interior of Sample No. 1 is nearly impervious to KOH unless it is vacuum filled. Thus it was probably not filled with electrolyte at the beginning of the test of TCP No. 1.

The poor ETU of Cell No. 1's ERP and consequent possibility of an underfill is at least a valid candidate for the mechanism responsible for the loss in dry side electrolyte concentration operating capability. Considering that the ERP probably increased in wettability over the life of the cell, it is very likely that the ERP started with very little electrolyte on the first fill, certainly less than 10 percent of capacity. The electrolyte found in the ERP's post test is quite low, $0.01 \text{ cm}^3/\text{cm}^2$ for Cell No. 1 and 0.08 for Cell No. 2. This agrees with the available wet volume measured for Cell No. 1, but is much lower than that for Cell No. 2, another anomalous result.

Initial work showed that many of the parts that had poor plating when completed could be detected by improved inspection techniques either before starting or part way through the process thus avoiding the expense of completing the part. However, trials to improve the degree of plating success by varying the concentrations of the several solutions in the process had no real impact. Some well-plated porous parts were obtained, but the process was not consistent. In some instances where plating appeared adequate on the outer surfaces, internal inspection showed virtually no plating penetration. In other cases, good internal plating was observed with poor external plating.

After exhausting the possible variables of concentration, exposure times, etc., efforts were made to replace the existing plating preparation solutions. Consultations with a plating firm resulted in replacement of the sensitizing and activating solutions with a combination sensitizer/activator followed by a post activator step. This appeared to have the result of making the sensitizing and activating steps more uniform since the results of plating immediately showed significant improvement. Plating of parts became considerably more consistent and the porosity as determined by the amount of water take up was significantly improved though still lower than desired. A high ERP porosity is desirable to provide the maximum volume of electrolyte available with the least weight and thickness of ERP.

To further improve the open porosity the porous polysulfone sinters were fabricated using a decreased amount of polysulfone powder. The polysulfone powder quantity was reduced from 12.5 gms to 9.6 gms for parts measuring 15 in. x 3.5 in. x 0.030 in. However, with this reduced quantity of material, difficulty was encountered in handling the polysulfone powder and the parts fabricated were considerably more fragile. To counteract this a new batch of

polysulfone powder was made (from polysulfone pellets) in which the ratio of polysulfone to methylene chloride solvent was increased by about 50 percent. The result was powder which was much more manageable and the structural integrity of the parts was improved. Results of porosity tests of the various batches of porous parts are shown in Table B-2.

TABLE B-2

POROSITY RESULTS

ERP WT' RANGE (GMS)	NO OF SAMPLES	APPARENT SOAK POROSITY % OPEN	APPARENT VACUUM POROSITY % OPEN	COMMENTS
12.7-13.0	6	29.4	39.84	
9.8-10.1	9	33.5	42.21	
8.7- 9.4	15	34.0	43.91	Extremely Fragile
9.3- 9.7	24	39.1	47.62	High ratio of P/S to Methylene chloride in powder prep

The vacuum porosity value shown in this table was obtained by immersing the part in water and applying 20 inches Hg vacuum to fill the part with water. Filled and dry weights were used to obtain the apparent porosity. As seen in Table B-2 the highest porosity was obtained with the samples in the 9.3-9.7 gram range. This weight ERP is now incorporated into the cell design.

The ERP water expulsion characteristics of the revised ERP fabrication and plating process compared to the original characteristics is shown in Figure B-1. The impact is that higher pressures are required to expell an equivalent amount of electrolyte in the new ERP's. This is considered to be an indication of improved internal plating as well as smaller mean pore size.

A further benefit of the increased electrolyte expulsion pressure characteristic is to allow a relaxing of reactant pressure control requirements when the cell configuration is incorporated into a power plant system.

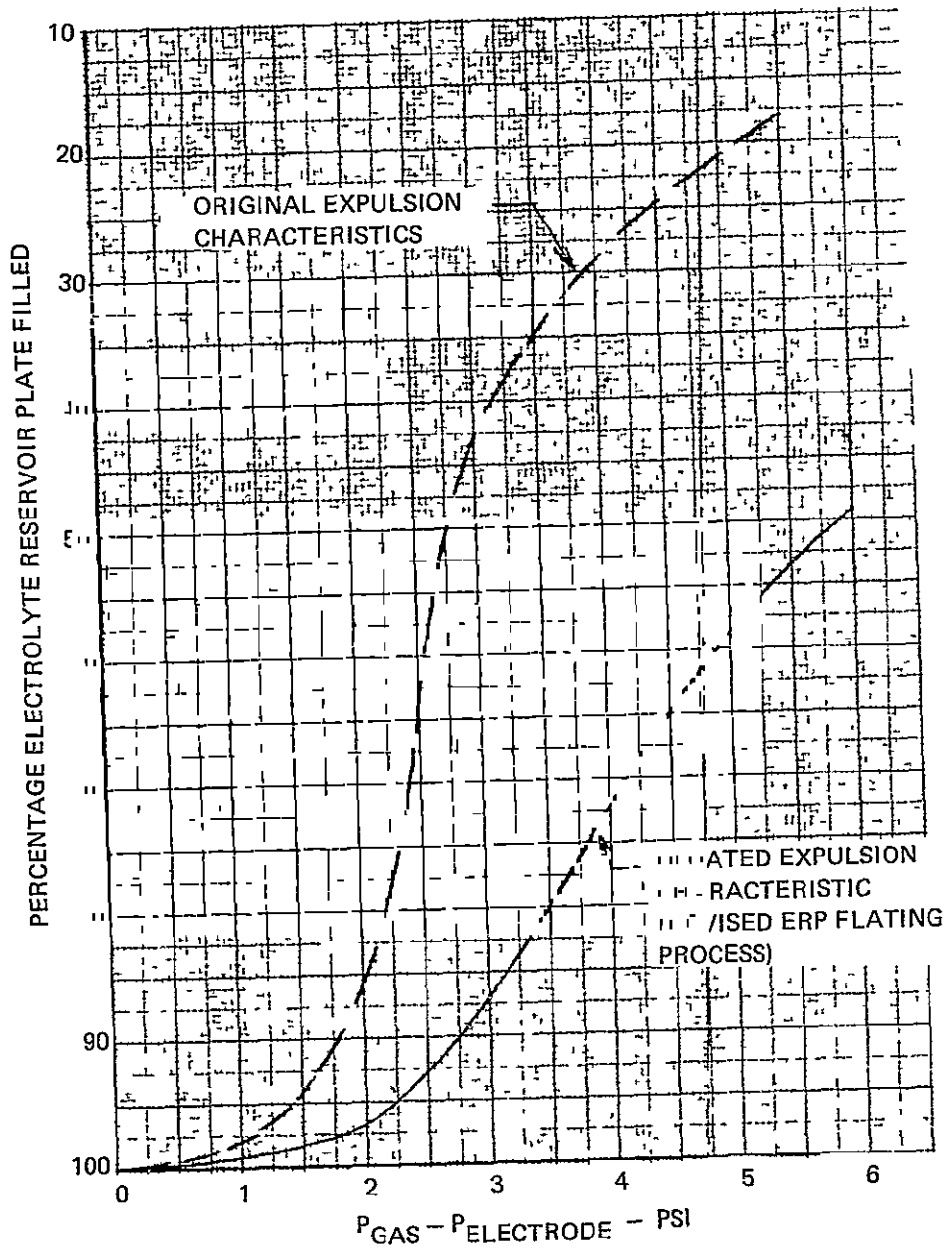


Figure B-1 — Water Expulsion Characteristics of Nickel-Plated Polysulfone Electrolyte Reservoir Plate

REFERENCES

- 1 Meyer, A. P., and Bell, W. F., "Development of Advanced Fuel Cell System (Phase IV) - Final Report", United Technologies Corporation, Power Systems Division, FCR-0165, NASA CR-135030, January 1976
- 2 Handley, L. M , Meyer, A P., Bell, W. F., "Development of Advanced Fuel Cell System (Phase III) - Final Report," United Aircraft Corporation, Pratt & Whitney Aircraft Division, PWA-5201, NASA CR134818, January 1975
- 3 Handley, L. M , Meyer, A. P., Bell, W. F., "Development of Advanced Fuel Cell System (Phase II) - Final Report, Pratt & Whitney Aircraft, PWA-4984, NASA CR134721
- 4 , Grevstad, P. E., "Development of Advanced Fuel Cell System" - Final Report, Pratt & Whitney Aircraft, PWA-4542, NASA CR-121136

APPENDIX C
NASA DISTRIBUTION LIST

NASA DISTRIBUTION LIST
FOR ELECTROCHEMICAL POWER REPORTS

NASA

Mr. Donald A. Beattie, Code R-14
National Aeronautics and Space
Administration
Washington, DC 20546

Mr. William Cunningham, Code KC
National Aeronautics and Space
Administration
Washington, DC 20546

Mr. Lee B. Holcomb, Code RPI
National Aeronautics and Space
Administration
Washington, DC 20546

Mr. James Lazar, Code RP
National Aeronautics and Space
Administration
Washington, DC 20546

Mr. Jerome P. Mullin, Code RPP
National Aeronautics and Space
Administration
Washington, DC 20546

National Aeronautics and Space
Administration
Scientific and Technical
Information Facility
P.O. Box 33
College Park, MD 20740

National Aeronautics and Space
Administration
Technology Utilization Office
Code KT
Washington, DC 20546

GODDARD

Mr. Floyd Ford, Code 711.2
Goddard Space Flight Center
National Aeronautics and Space
Administration
Greenbelt, MD 20771

Mr. Dale W. Harris, Code 711 0
Goddard Space Flight Center
National Aeronautics and Space
Administration
Greenbelt, MD 20771

JOHNSON

Mr. Hoyt McBryar, EP5 (3 copies)
Johnson Space Center
National Aeronautics and Space
Administration
Houston, TX 77058

Mr. Barry Trout, EP5
Johnson Space Center
National Aeronautics and Space
Administration
Houston, TX 77058

LEWIS

Dr. J. Stuart Fordyce, MS 302-1
Lewis Research Center
National Aeronautics and Space
Administration
21000 Brookpark Road
Cleveland, OH 44135

Dr. Robert E. Post
Lewis Research Center
National Aeronautics and Space
Administration
2100 Brookpark Road
Cleveland, OH 44135

Mr. Paul Prokopius, MS 309-1
Lewis Research Center
National Aeronautics and Space
Administration
21000 Brookpark Road
Cleveland, OH 44135

Dr. Louis Rosenblum, MS 49-5
Lewis Research Center
National Aeronautics and Space
Administration
21000 Brookpark Road
Cleveland, OH 44135

Dr. Marvin Warshay, MS 302-1
Lewis Research Center
National Aeronautics and Space
Administration
21000 Brookpark Road
Cleveland, OH 44135

MARSHALL

Mr. Pete George, EC-12
George C. Marshall Space Flight
Center
National Aeronautics and Space
Administration
Huntsville, AL 35812

Mr. J. L. Miller, EC-12
George C. Marshall Space
Flight Center
National Aeronautics and Space
Administration
Huntsville, AL 35812

Mr. Etheridge Paschal, EC-12
George C. Marshall Space
Flight Center
National Aeronautics and Space
Administration
Huntsville, AL 35812

JET PROPULSION LABORATORY

Mr. Aiji A. Uchiyama
MS 198-220
Jet Propulsion Laboratory
4800 Oak Grove Drive
Pasadena, CA 91103

AIR FORCE

Mr. D. Pickett AFAPL/POE-1
Aero Propulsion Laboratory
Wright Patterson AFB, OH 45433

Mr. D. R. Warnock/AFAPL/POE
Wright Patterson AFB, OH 45433

Air Force Aero Propulsion Lab
POE-1, W.S. Bishop
Wright Patterson AFB, OH 45433

SAMSO/DYAE
P.O. Box 92960
Worldway Postal Center
Los Angeles, CA 90009

ARMY

Harry Diamond Laboratories
ATTN: A. A. Binderly
Room 300, Building 92
Connecticut Ave & Van Ness St NW
Washington, DC 20438

Commanding Officer
U. S. Army Mobility Equipment
Research & Development Center
Electrotechnology Department
Electrochemical Division
ATTN: SMEFB-EE
Fort Belvoir, VA 22061

U. S. Army Electronics Command
ATTN: AMSEL-TL-P
Fort Manmouth, N. J. 07703

NAVY

Mr. Albert Henny, 6157D
Naval Ship Engineering Center
Center Bldg., Prince Georges
Center
Hyattsville, MD 20782

Mr. J. A. Woerner
Naval Ship R&D Center
Annapolis, MD 21402

Naval Surface Weapons Center
Electrochemistry Division, Code 232
White Oaks, MD 20910

PRIVATE ORGANIZATIONS

Mr. R. L. Beauchamp
Bell Telephone Laboratories
Murray Hill, NJ 07940

Dr. James D. Birkett
Arthur D. Little, Inc.
Acorn Park
Cambridge, MA 02140

Mr. E. P. Broglio
Eagle Picher Industries, Inc.
P. O. Box 47, Couples Dept.
Joplin, MO 64801

Dr. J. G. Cohn
Engelhard Industries
Menlo Park
Edison, NJ 08817

Mr. James Dunlop
COMSAT Laboratories
Clarksburg, MD 20734

Mr. D. O. Feder, RM 1E-247
Bell Telephone Laboratories, Inc.
Murray Hill, NJ 07974

Mr. R. F. Fogle, GA 42
Rockwell International Corp.
Autonetics Division
3370 Miraloma Ave.
Anaheim, CA 92803

Dr. R. T. Foley
Chemistry Department
American University
Massachusetts & Nebraska Ave NW
Washington, DC 20016

Mr. Larry Gibson
Aerospace Corporation
P.O. Box 95085
Los Angeles, CA 90045

Mr. Sidney Gross MS 8E-37
The Boeing Company
P.O. Box 3999
Seattle, Washington 98124

Mr. R. Hamilton
Institute for Defense Analyses
400 Army-Navy Drive
Arlington, VA 22202

Dr. E. A. Heintz
Technical Department
Airco Speer Carbon Graphite
P.O. Box 828
Niagara Falls, NY 14302

Dr. Fritz R. Kalhammer
Electric Power Research Institute
Box 10412
Palo Alto, CA 94304